In vitro testing of the predicted viral fitness landscape for the HIV-1 Nef protein

---

Submitted by:

Erasha Rajkoomar

In fulfilment of the requirements for the degree of

Master in Medical Sciences in Virology

Faculty of Health Sciences

University of KwaZulu-Natal

2015

TABLE OF CONTENTS

PREFACE

The experimental work described in this dissertation was carried out in the Hasso Plattner Research Laboratory, HIV Pathogenesis Programme Laboratory, and Africa Centre Laboratory, in the Doris Duke Medical Research Institute, Nelson R. Mandela School of Medicine, University of KwaZulu-Natal, Durban, from February 2013 to June 2015, under the supervision of Dr. Jaclyn Mann and Prof. Thumbi Ndung'u.

These studies represent original work by the author and have not otherwise been submitted in any form for any degree or diploma to any other University. Where use has been made of the work of others, it is duly acknowledged in the text.

_____ _____

Erasha Rajkoomar (Student) Date

_____ _____

Dr. Jaclyn Mann (Supervisor) Date

_____ _____

Prof. Thumbi Ndung'u (Co-supervisor) Date

DECLARATION

I, Erasha Rajkoomar, declare that:

(i) The research reported in this dissertation, except otherwise indicated, is my original work.

(ii) This dissertation has not been submitted for any degree or examination at any other university.

(iii) This dissertation does not contain other person's data, pictures, graphs or other information, unless specifically acknowledged as being sourced from other persons.

(iv) This dissertation does not contain other person's writing, unless specifically acknowledged as being sourced from other researchers. Where other written sources have been quoted, then:

a. Their words have been re-written but the general information attributed to them has been referenced.

b. Where their exact words have been used, their writing has been placed inside quotation marks and referenced.

(v) Where I have reproduced a publication of which I am an author, co-author or editor, I have indicated in detail which part of the publication was written by myself alone and have fully referenced such publications.

(vi) This dissertation does not contain text, graphics or tables copied and pasted from the internet unless specifically acknowledged, and the source being detailed in the dissertation and in the references section.

Signed _____ Date _____

ACKNOWLEDGEMENTS

I would like to thank:

- Dr. Jaclyn Mann for her supervision, support, patience, guidance, willingness to help and enthusiasm throughout the project
- Prof. Thumbi Ndung'u for his supervision and guidance
- Saleha Omarjee for teaching me the experimental procedures
- Staff and students at the HIV Pathogenesis Programme
- Collaborators of the study
- The National Research Foundation and Howard Hughes Medical Institute for funding

ABSTRACT

An effective vaccine against HIV-1 remains elusive and this is mainly due to the ability of the virus to readily mutate and evade immune responses. Computational models, namely Ising and Potts, have been developed, using methods from physics, with the ability to predict the viral fitness landscapes of different HIV-1 proteins. This could reveal vulnerabilities within the proteins which may indicate regions suitable for inclusion in a HIV vaccine that aims to corner the virus and block immune escape. These models were previously validated by testing *in vitro* the viral fitness landscape for the Gag protein. Even though Nef is an important HIV-1 virulence factor, the predicted viral fitness landscape for the Nef protein has not yet been tested. The present study aimed to evaluate the accuracy of these computational models in predicting the fitness consequences of mutations in HIV-1 Nef, by measuring the Nef-driven replication capacities as well as CD4 and HLA down-modulation capacities of 32 different Nef mutants. Mutants were selected that had a wide range of energy (E) values (predicted fitness where high E values are expected to correspond to low fitness and low E values are expected to correspond to high fitness) and were created by site-directed mutagenesis of a NL4-3 plasmid encoding the consensus B Nef sequence. Virus stocks were generated by transfection of a GXR cell line with mutant plasmids and replication capacities of the viruses were then measured in peripheral blood mononuclear cells using p24 ELISA. Additionally, CD4 and HLA down-modulation capacities of the mutant Nefs were measured by transfecting a GXR cell line modified to express high levels of HLA-A*02 with the mutant Nef sequences that were cloned into a pselect plasmid, followed by staining with fluorochrome-conjugated CD4 and HLA-A*02 antibodies and measurement of the level of cell-surface expression of these molecules by flow cytometry. The E values predicted by both the Ising and Potts models correlated significantly with Nef-driven

replication capacities (Ising: r = –0.5793, p = 0.0006 and Potts: r = –0.4118, p = 0.0213) and CD4 down-modulation capacities (Ising: r = –0.5266, p = 0.0023 and Potts: r = –0.3781, p = 0.0360, but not HLA-A*02 down-modulation capacities (Ising: p = 0.8530 and Potts: p = 0.3676), of the various Nef mutants. The experimental data supports the predictions of both the Ising and Potts models, however, the Ising model proved to more accurately predict fitness consequences of mutations in the Nef protein. Model predictions for Nef were not as accurate, however, as for the highly conserved Gag protein. In addition, the data suggests that Nef-driven replication capacity and CD4 down-modulation may be more important functions of Nef *in vivo* than HLA down-modulation. Overall, our data supports computational modelling as a valid approach to rational immunogen design.

CHAPTER 1

INTRODUCTION

1.1 Overview

The causative agent of acquired immune deficiency syndrome (AIDS), a syndrome of opportunistic infections and cancers, is the retrovirus human immunodeficiency virus (HIV) which infects human immune cells expressing the CD4 antigen (11, 47, 114). HIV type 1 (HIV-1) causes the vast majority of HIV infections (11, 47). HIV/AIDS is a global pandemic, with almost seventy million people infected since its initial identification and approximately thirty five million people were living with HIV at the end of 2013 (158).

Currently, HIV-1 is treated with antiretroviral therapy which increases the life expectancy of infected individuals (14). However, this treatment is associated with several limitations including a high cost factor (95). In addition it is improbable that the virus will be eradicated with antiretroviral therapy in areas where the epidemic is rife (112). The most affordable and efficient way in eliminating HIV-1 is through the development of an effective vaccine against the virus (5). Despite immense efforts in developing an effective vaccine, attempts thus far remain unsuccessful (112). One vaccine however showed partial success in protection against HIV infection, but it is not sufficiently efficacious (137). The major hurdle in vaccine design and development is eliciting a human immune response that is not evaded by the highly diverse and mutable HIV-1 (5, 85, 164). Thus, new strategies are required for the production of an effective HIV-1 vaccine.

This review will highlight the structure and replication cycle of HIV-1. Additionally, HIV-1 pathogenesis and immune evasion strategies will be discussed. Current treatment and

preventative measures as well as challenges in HIV-1 vaccine design will be briefly outlined. Throughout the review, there will be an emphasis on Nef since it is critical to HIV-1 pathogenesis and host immune evasion and is the focus of the current project. Finally, a new vaccine strategy that uses computational models predicting the viral fitness landscape of HIV-1 proteins to aid in vaccine immunogen design will be discussed followed by an introduction of the aim of the present project to test the accuracy of these models in predicting the fitness landscape for the HIV-1 Nef protein.

1.2 Genome and Structure of HIV-1

1.2.1 Genome organisation

The HIV-1 genome encodes nine genes namely group specific antigen (*gag*), polymerase (*pol*), envelope (*env*), transactivator of transcription factor (*tat*), regulator of virion protein (*rev*), negative regulatory factor (*nef*), viral infectivity factor, (*vif*), viral protein R (*vpr*) and viral protein U (*vpu*) (54, 156). Gag, Pol, and Env polyproteins ($Pr55^{Gag}$, $Pr160^{GagPol}$ and gp160, respectively) are proteolysed into individual proteins (54). $Pr55^{Gag}$ is cleaved by the viral protease (PR) to Gag protein matrix (MA/p17), capsid (CA/p24), nucleocapsid (NC/p7) and p6 as well as two spacer peptides (p1 and p2) (55, 153). In addition, $Pr160^{GagPol}$ is cleaved by the viral PR to form the enzymes reverse transcriptase (RT) and integrase (IN) (55, 153). The Env polyprotein precursor is cleaved by a cellular protease and results in the generation of the surface unit (SU) Env glycoprotein, gp120, and the transmembrane (TM) glycoprotein, gp41 (55). Nef, Vif, Vpu, and Vpr are termed accessory proteins as they were, initially, not thought to be essential for infection (142). However, it is now known that these proteins are involved in

multiple mechanisms of immune evasion (103). Tat and Rev are regulatory proteins required for transcription and viral RNA transport, respectively (55).

1.2.2 Structure

HIV particles are typically sphere shaped and have a diameter of approximately 120 nm (16, 84). The envelope, containing viral glycoproteins, constitutes the virion outer layer and is of cellular origin (120). HIV envelope spikes are composed of three gp120 and gp41 glycoproteins each (72). Within the viral envelope is a conical-shaped core particle which encompasses the viral genome and replication proteins (58). The outer shell of this core, is formed by the Gag p17 matrix molecules, and surrounds Gag p24 capsid molecules (110). The Gag p24 capsid encloses a ribonucleoprotein (RNP) complex with two copies of single-stranded genomic ribonucleic acid (RNA) which interact with each other and are associated with Gag p7 nucleocapsid molecules (32, 65, 120). Additionally, PR, RT and IN are encased in the nucleocapsid (65).

1.3 HIV-1 replication cycle

HIV-1 replication occurs through a series of steps (Figure 1.1): (i) viral entry, (ii) reverse transcription, (iii) uncoating and nuclear import, (iv) proviral DNA integration, (v) transcription and nuclear export, (vi) assembly and budding, (vii) maturation; and a brief description of each step follows. In addition, the role of Nef at several steps during the virus replication cycle is discussed.

Figure 1.1. HIV-1 replication cycle (modified from AIDSinfo [www.aidsinfo.nih.gov] (3))

The diagram represents the mechanistic steps involved in HIV-1 replication: 1 – virus entry by binding and fusion, 2 – reverse transcription of HIV-1 RNA, 3 – nuclear import, 4 – integration of viral DNA, 5 – transcription and nuclear export, 6 – assembly and budding, 7 – maturation, respectively.

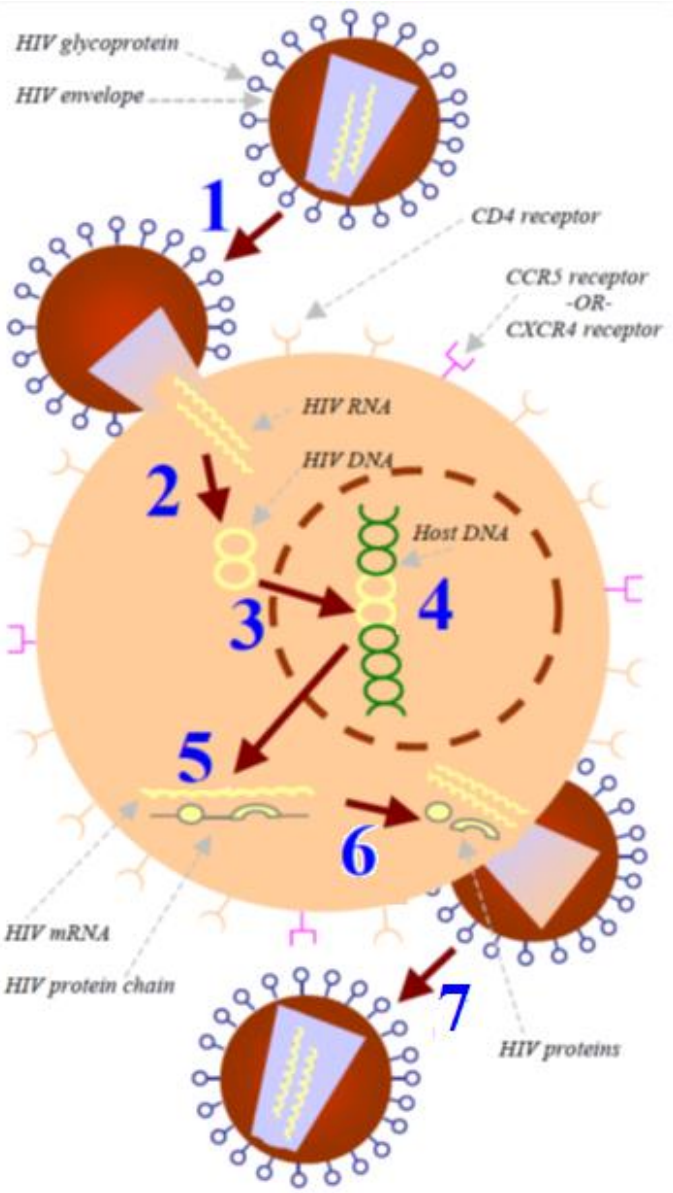
HIV glycoprotein
HIV envelope
1
CD4 receptor
CCR5 receptor
-OR-
CXCR4 receptor
HIV RNA
HIV DNA
2
Host DNA
3
4
5
6
HIV mRNA
HIV protein chain
7
HIV proteins

1.3.1 Viral entry

HIV-1 gp120, binds to CD4 (known as the primary receptor), which may be present on the surface of helper T cells, memory T cells, macrophages, monocytes, dendritic cells and Langerhans cells (37, 46, 86). Once gp120 has bound to the CD4 receptor, it changes conformation to allow for binding of secondary/co-receptors, most commonly C-C chemokine receptor 5 (CCR5) or the CXC chemokine receptor 4 (CXCR4) (13, 43). Upon co-receptor attachment, glycoprotein (gp41) interacts with the membrane of the target cell through the formation of a triple-stranded coiled-coil (108). This consequently leads to the development of a six-helix bundle and ultimately to the formation of a fusion pore which in turn leads to the fusion of the virus and the target cell membranes (108, 115).

Once the fusion of host cell and virion occurs, the HIV-1 genome needs to be integrated into the genome of the host cell (63). In order for integration to occur, it is first required that the single-stranded RNA be converted to double-stranded proviral DNA and this is accomplished through a process called reverse transcription (63).

1.3.2 Reverse transcription

Firstly, host cell $tRNA^{Lys3}$ anneals to the 5'-end of the primer binding site (PBS) of the HIV-1 viral RNA template (71). The tRNA/RNA complex is then recognised by RT which extends the 3'-end of the annealed primer thereby initiating reverse transcription (63). A segment of minus strand DNA is produced when RT completes synthesis at the 5'-end of genomic DNA (71). RNase H then degrades the 5' end of the RNA releasing minus strand DNA which binds to the 3'-

end of the RNA and initiates minus strand DNA synthesis from this end (termed first strand transfer) (63, 71). As minus strand DNA is produced, RNase H cleaves the RNA template creating RNA primers which are used for the formation of two plus strand RNA fragments (71). RNase H cleaves and displaces tRNA from the PBS leaving complementary plus and minus PBS DNA strands that hybridise and allow DNA synthesis to resume to completion (63).

The last step in HIV-1 reverse transcription is DNA flap formation (9). This event in reverse transcription promotes uncoating of HIV-1 at the nuclear pore (9).

1.3.3 Uncoating and nuclear import

Before entry of the viral genome into the nucleus of an infected cell, the virus loses its viral capsid by a process termed uncoating (8). The mechanism of HIV-1 uncoating is poorly understood but it is required for the next step in the viral replication cycle, i.e. nuclear import (163). During nuclear import, it accompanies the transition from reverse transcriptase complexes [(RTCs) in which RT takes place] to pre-integration complexes (PICs) which are competent for integration into the host genome (8, 9).

1.3.4 Proviral DNA integration

Viral integrase which enters the host cell as part of the virion, catalyses the reactions required for successful integration of HIV-1 DNA into the host genome (152). The 3'-ends of the viral DNA are cleaved and ligated to the 5'-ends of the similarly cleaved host target DNA (152). Ligation

results in a gapped product which is then repaired by the host cell DNA repair enzymes (152). It has been shown that several host cellular proteins and other HIV-1 proteins, some of which form part of the PICs, are required for successful proviral DNA integration into the host DNA (97).

The integrated proviral genome needs to be transcribed for the production of progeny virions and occurs through a process termed transcription (138).

1.3.5 Transcription and nuclear export

HIV-1 transcription depends on interactions between several host cell factors and the viral Tat protein (126). Tat recognises a trans-activation responsive element region (TAR) and recruits the cellular positive transcription elongation factor (P-TEFb) which increases binding of TAR to the Tat activation domain (126). The Tat/TAR interaction, in turn, recruits one component of PTEFb, CDK9 (a cyclin-dependent kinase), which phosphorylates the carboxy-terminal domain of the host cell RNA polymerase II (RNAPII) stimulating elongation (45). Completely and incompletely spliced RNA species (encoding for viral proteins) as well as full length RNA species (which constitutes the viral genome) are transcribed (126). Rev is involved in exporting these RNA species into the cytoplasm, where they are translated into the HIV-1 proteins (126).

1.3.6 Assembly and budding

During trafficking of the Env glycoprotein to the plasma membrane, it is matured into gp120 and gp41 subunits by the cellular protein furin (121). The Gag polyprotein, $pr55^{Gag}$, synthesised on

free ribosomes, associates with the Env glycoproteins in lipid rafts of the plasma membrane where assembly transpires (94). Specifically, the Gag matrix domain interaction with Env gp41 results in incorporation of Env proteins into virions (61, 129). The Gag nucleocapsid region of the Gag polyprotein binds and transports viral genomic RNA to the plasma membrane where Gag multimerisation follows (129). Once enough Gag subunits are produced, a viral capsid is formed, which encloses the viral genomic RNA, viral proteins and cellular proteins (121). Completion of virion assembly leads to subsequent budding.

Budding of HIV-1 is initiated when domains in Gag p6, for example the PTAP motif, interact with cellular machinery termed endosomal sorting complexes required for transport (ESCRT) (94, 121). Viral maturation is the succeeding step and is critical in viral infectivity (88).

1.3.7 Maturation

A mature virion is produced when viral protease cleaves the Gag and Gag-Pol precursors upon budding (61). Upon maturation, while the Gag matrix protein remains associated with the viral envelope, the Gag capsid molecules reassemble to form a conical core which encloses the nucleocapsid, genomic dimeric RNA as well as viral and cellular proteins (88). After virion maturation, the viral replication cycle is compete and the virus is rendered infectious (162).

1.4 HIV-1 replication cycle: role of Nef

HIV-1 Nef is a small myristoylated protein (~27kDa), usually, with a length of 206 amino acids (51). Nef has a structured core, flexible N and C termini and an internal flexible loop (52). This HIV-1 protein serves in several stages of the viral life cycle and is required for optimal viral replication (64). Nef enhances viral replication through a number of strategies/activities, which will be discussed next. Major functional motifs involved in these activities are summarised in Table 1.1.

1.4.1 Nef-mediated CD4 down-modulation

Nef-mediated CD4 down-modulation occurs early after viral infection and prevents the acquisition of unfavorable viral superinfections which may lead to premature cell death thereby enhancing HIV replication (64). In addition, Env sequestration into a CD4/Env complex which would result in impaired virion infectivity is avoided by CD4 down-modulation as it enables progeny virions to incorporate higher amounts of Env products (thus becoming more infectious) (125). Another benefit to the virus would be an expected increase in the release of viral particles as high levels of surface CD4 have been shown to interfere with the budding of virions (64). For CD4 down-modulation, Nef (amino acids 57 – 59, 95, 97, 106 and 110) binds to the CD4 cytoplasmic tail (64) (Table1). In addition, the dileucine (EXXXLL extending from amino acids 160 – 165) and diacidic ([E/D]D from amino acids 174 – 175) residues present in Nef allows for binding of the AP-2 which recruits proteins for CD4 internalisation in clathrin-coated pits (38, 51, 64) (Table 1.1).

Table 1.1. Nef motifs and related functions

Motif	Codon	Function
MGxxxS	1 – 6	Signals Nef myristoylation for cellular membrane targeting and plays and important role in all Nef functions
WLE, G, L, R, L	57 – 59, 95, 97, 106, 110	Binds to the cytoplasmic tail of CD4, which is required for CD4 down-modulation
EEEE	62 – 65	This motif mimics an acidic cluster which binds to PACS-1. Through this PACS-1 binding ability, Nef may stimulate a signaling pathway for the down-regulation of HLA-I. Additionally, it is important for PAK2 activation and enhanced infectivity
PxxPxR	72 – 77	This is a SH3 binding region and is required for PAK2 activation, HLA-I down-modulation and enhanced virion infectivity
RR	105 – 106	This is a highly conserved Nef motif which induces PAK2 activation. In addition it is suggestive that this site is functional in CD4 and HLA-I down-modulation
FPD	121 – 123	This motif plays a role in several Nef functions, namely, CD4 down-modulation, HLA-I down-modulation, PAK2 activation and enhancement of viral infectivity
ExxxLL **[E/D]D**	160 – 165 174 – 175	These motifs bind to adaptor proteins to enable CD4 down-modulation

Information provided in the table was sourced from (52) and (60).

1.4.2 Nef-driven infectivity: early stage of the life cycle

Nef increases the infectivity of HIV-1 not only through CD4-dependent mechanisms, as described above, but also through CD4-independent mechanisms which are not well understood (4, 25). A study showed that viruses mutated in *nef* are four to 40 times less infectious than wild-type HIV-1 in a single-round of infection (4). It was also shown that these *nef*-defective virions bind and enter the target cells efficiently, however once inside the cell these viruses are restricted in their ability to reverse transcribe their genomes, all suggestive of a role of Nef at an early post-entry stage in the viral replication cycle before reverse transcription (4, 25). It has been suggested that Nef might modify the virus core following entry, making it more competent for viral DNA synthesis (4).

1.4.3 Nef-mediated cellular activation

HIV-1 replication is restricted in resting T cells and ensues once the cells are activated (128). Nef induces cell activation by lowering the threshold required for T cell receptor (TCR) stimulation through its interaction with cell signaling molecules (128). Nef activation of p21 activated kinase 2 (PAK2) is a well described Nef activity (51). Activation of PAK2 by Nef is stimulated when Nef (RR motif; amino acids 105 – 106) forms a complex with this molecule (51) (Table 1.1). It is known that the Nef/PAK2 association induces T cell activation but the complex remains uncharacterised (128). It has been shown that in sub-maximally activated T cells, viruses defective for Nef/PAK2 association, but not other Nef functions, did not enhance replication and, it was therefore suggested that Nef/PAK2 association is important for Nef-mediated enhancement of HIV-1 replication (128).

In addition to the aforementioned strategies used by Nef to directly enhance HIV-1 replication, Nef can promote immune evasion through human leukocyte antigen (HLA)-I down-modulation and therefore indirectly enhance virus replication. A discussion on this function of Nef follows in the section on HIV-1 immune evasion (Section 1.5.4.2.3).

1.5 HIV-1 pathogenesis

Transmission of HIV-1 is a consequence of exposure to blood, a blood product or bodily secretion that have been contaminated with the virus (34). HIV-1 is dominantly transmitted sexually (oral, vaginal or anal), as well as less frequently, parenterally (drug use and blood transfusion) and vertically (mother to child transmission - before, during or after birth and through breast milk) (36). Once transmitted, the progression of HIV-1 to AIDS is intermediated by a series of stages, namely primary and chronic stages (79) (Figure 1.2). The aforementioned stages are briefly outlined.

1.5.1 Primary phase

The primary stage of infection is considered to be from the time of virus exposure until seroconversion (76). The first cells to be infected with the virus are primarily $CD4^+$ $CCR5^+$ memory T cells (44) as well as other cell types including Langerhans (mucosal dendritic cells [DCs]) and macrophages (68, 145). Following transmission there is an initial period in which infection is established at the site of exposure but diffusion in the systemic circulation is not detectable (35) and this period is termed the eclipse phase (Figure 1.2).

Figure 1.2. HIV-1 pathogenesis (based on original from Pantaleo *et al.* (132))

The graph depicts the various stages of HIV-1 infection (primary [eclipse and acute], chronic and AIDS) and the approximate corresponding time periods associated with each stage. In addition, the $CD4^+$ T lymphocyte count and HIV plasma viral load level associated with each stage of infection is shown.

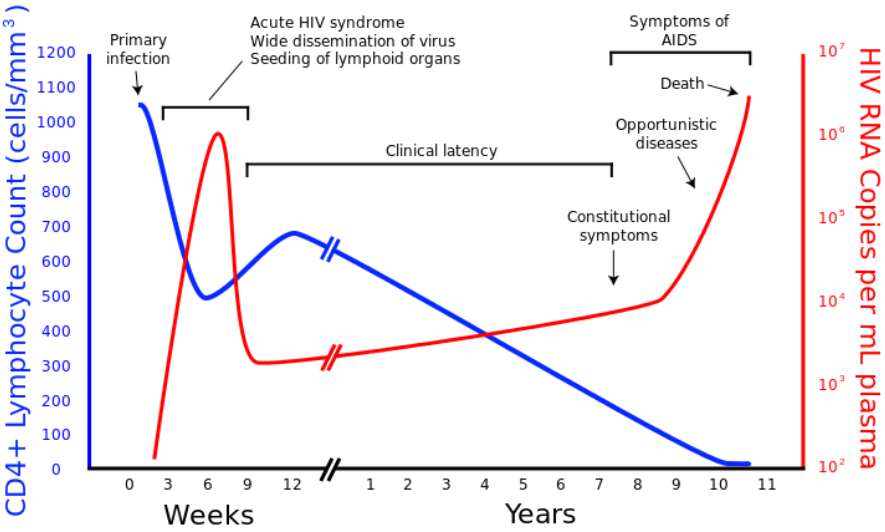
CD4+ Lymphocyte Count (cells/mm³)
HIV RNA Copies per mL plasma
Primary infection
Acute HIV syndrome
Wide dissemination of virus
Seeding of lymphoid organs
Clinical latency
Symptoms of AIDS
Death
Opportunistic diseases
Constitutional symptoms
Weeks
Years

It has been demonstrated that a reservoir of latently infected cells ($CD4^+$ T cells, DCs and macrophages) is established during this phase (157). This early establishment allows for lifelong persistence of HIV-1 as latent cells are not recognised by the immune system and are infectious upon cell re-activation (50).

Following the eclipse phase (approximately 10 days in duration) is the acute phase (Figure 1.2) during which the virus enters systemic circulation and infects a greater number of $CD4^+$ T cells in lymphoid tissue, including the lymph node (44) as well as bone marrow (35). Establishment of infection in the lymphoid tissues leads to the virus replicating rapidly (68). A threshold of replication is reached within 21-28 days post-infection, corresponding to peak plasma viraemia (154) (Figure 1.2). The peak viraemia may be one to 10 million HIV-1 RNA copies/ml plasma and is accompanied by a steep decline in the number of CD4 T cells (68). Furthermore, during this stage of infection 50 to 90 percent of individuals display ailments common to other illnesses, such as fever, rash, malaise, sore throat and joint pain (30, 68). During this time frame, the patient is highly infectious (44).

1.5.2 Chronic phase

There is an unstable interplay between HIV-1 replication and the host immune responses during the chronic phase of infection (44). During chronic infection, a state of chronic immune activation is reached due to the constant viral replication (44) and as a result of many stimuli including direct activation of T cells via viral constituents Nef (described in Section 1.5.4.1.2) and gp120, virally stimulated production of circulating pro-inflammatory cytokines and bacterial

translocation across the mucosal barrier (15, 117). In addition to HIV-1 infection induced CD4+ T cell decline, immune activation adds to the gradual loss in the number of CD4+ T cells via activation-induced cell death (44, 48). Since $CD4^+$ T cells play a vital role in the immune system (101), their decline leads to a lowered immune response. Progressive immune degradation reduces the immune system's ability to replenish depleted $CD4^+$ T cells (48). HIV-1, however, remains persistent and continuously drives the proliferation and depletion of $CD8^+$ T cells which in turn leads to further depletion of $CD4^+$ T cells (24). Viral replication increases progressively, slowly reaching the end of the chronic phase of infection, which, on average, lasts for a duration of seven to 10 years (70).

1.5.3 AIDS

Once a hosts $CD4^+$ T cells decline below the threshold of approximately 200 cells/mm^3, the host becomes immune-deficient and susceptible to opportunistic illnesses which ultimately results in death as the immune system eventually collapses (154). Pulmonary parenchymal complications are the main cause of illness and death in patients with AIDS and include pneumonias, tuberculosis and non-tuberculous mycobacteria (31). Other leading causes of death in AIDS patients include esophageal candidiasis and cervical cancer (20).

1.5.4 Host immune responses: role of Nef in immune evasion

Several innate and adaptive responses are elicited by the host immune system to control and eliminate HIV-1 infection. However, elimination of the virus through these immune responses is generally unsuccessful due to the virus's ability to evade these responses or use them to drive

disease progression. Each of these responses are outlined below and the significant contribution of Nef to immune evasion is discussed.

1.5.4.1 Innate immunity

The innate immune system constitutes the first line of defense against invading pathogens, including HIV-1 and involves the action of host restriction factors and cells such as macrophages, dendritic cells and natural killer cells (117).

1.5.4.1.1 Host restriction factors

Host restriction factors interfere with different stages of the viral life cycle: apolipoprotein B mRNA-editing, enzyme-catalytic, polypeptide-like 3G (APOBEC3G) induces lethal hypermutations of newly synthesised HIV-1 DNA; tripartite motif-containing protein 5 alpha (TRIM5α) restricts the incoming retroviral capsid; and tetherin restricts budding of virions from infected cells (75, 102). HIV-1 proteins Vif and Vpu counteract APOBEC3G and tetherin, respectively (102). A role for HIV-1 Nef in counteracting these host restriction factors has not been described.

1.5.4.1.2 Macrophages and dendritic cells

One of the first cell types to recognise pathogens are macrophages, which consequently ingest these pathogens and elicit a T cell immune response through cytokine signalling and antigen presentation (87). Dendritic cells are also among the first immune cells to encounter HIV

following infection and they, like macrophages, are involved in T cell activation (87, 113). Macrophages and dendritic cells present HIV-1 peptides, via the HLA-II pathway, to $CD4^+$ T cells thereby triggering $CD4^+$ T helper responses that are required for anti-HIV antibody and cytotoxic T lymphocyte (CTL) immune responses (82, 119).

HIV-1, however, infects macrophages and dendritic cells and has evolved mechanisms to counter their responses as well as utilise and manipulate these cells to assist HIV-1 disease progression (82, 119). For example, HIV-1 Nef prolongs the life span of infected macrophages and, stimulates macrophages to secrete factors that permit the infection of resting T cells, actions which increase the latent reservoir (59, 82, 147). Nef also shifts macrophages from an anti-inflammatory to an active pro-inflammatory phenotype and this contributes to chronic immune activation (27).

Furthermore, Nef impairs antigen presentation by disrupting HLA-II surface expression thereby reducing the presentation of foreign peptides to CD4 cells which would otherwise be activated (41).

1.5.4.1.3 Natural killer (NK) cells

NK cell antiviral capability is due to their production of cytokines, immunoregulatory effects on cells or by cytolytic activity (131). During HIV-1 infection, NK cells release macrophage inflammatory proteins (such as MIP-1-α) and other chemokines which suppress replication of R5

strains of HIV by competing with HIV for CCR5 (111). NK cell cytolytic activity is under the control of activating and inhibiting killer immunoglobulin (Ig)-like receptors (KIRs) which, upon binding of specific HLA molecules, will determine inhibition or activation of cytolysis (131). The binding of HLA-C and HLA-E molecules by KIRs, for example, inhibits NK cell-mediated killing (26). Nef mediates evasion of NK cell-mediated killing of infected cells through selective down-modulation of HLA-A and HLA-B molecules, but not HLA-C and HLA-E molecules, from the surface of infected cells (33). The mechanism of Nef-mediated down-modulation of HLA molecules as well as Nef's involvement in evasion of CTL responses will be subsequently discussed (Section 1.5.4.2.3).

1.5.4.2 Adaptive immunity

1.5.4.2.1 $CD4^+$ T cells

$CD4^+$ T cells play a central role in immune control by helping both $CD8^+$ T cells and B cells in infection eradication through stimulating the differentiation and proliferation of these cells once they have encountered an antigen (101). As described earlier (Section 1.5.4.1.2), antigen-presenting cells present anti-HIV peptides to $CD4^+$ T cells which results in their activation, however Nef has the ability to disrupt antigen presentation thus contributing to the impairment of $CD4^+$ T cell responses. HIV-1 also infects and destroys $CD4^+$ T cells, thereby weakening the overall effect of the immune system (66). Nef makes a significant contribution to this depletion of $CD4^+$ T cells: indeed, it has been shown, in the SCID-hu mouse model, that infection with HIV_{NL4-3} mutants with defective *nef* did not result in/or resulted in minor depletion of $CD4^+$ T cells (74). Nef increases the expression of the Fas ligand (CD95L) on infected cells, which in

turn increases Fas-mediated apoptosis upon bystander Fas (CD95) binding thereby indirectly destroying bystander T cells (6, 41). Additionally, Nef triggers apoptosis by inducing the release of exosomes from T cells, used for the transport of extracellular Nef, which causes activation induced cell death in these bystander cells (90).

Since $CD4^+$ T cells are involved in the differentiation and proliferation of B cells and $CD8^+$ T cells, their depletion indirectly impairs B cell and $CD8^+$ T cell immune responses.

1.5.4.2.2 B cells

B cells are activated upon exposure to an antigen and consequently secrete specific antibodies (140). Non-neutralising antibodies are present in large amounts throughout viral infection but this has only a small effect on HIV-1 infectivity (159). Neutralising antibodies (Nab) develop slowly and may have an effect on HIV-1 infectivity, however, Nab responses may be ineffective against the rapidly mutating virus (mutations arise as a result of error prone RT) (140). The Nab responses exerts a selective pressure that drives continuous evolution of neutralisation escape mutants to which new Nab responses must be generated, thus the Nab response lags behind virus evolution (155). HIV may also directly impair the B cell response. For example, it has been shown that in infected macrophages, Nef induces the formation of specific channels to mediate its own transfer to neighboring B cells which results in impaired antibody responses in these cells (80).

1.5.4.2.3 $CD8^+$ T cells

The suppression of HIV-1 during early infection, which culminates the primary stage of HIV-1 infection, is due to $CD8^+$ T cell or CTL-mediated selective pressure (83, 135). During primary infection, there is a simultaneous decline in viremia and increase in CTL-induced anti-HIV responses (135). CTLs recognise HIV-1 epitopes presented by HLA-I molecules on the surface of infected cells (33). The infected cells are subsequently killed through CTL insertion of perforin pores in the cell membrane which allows for the entry of enzymes (granzymes) that in turn activate a death program leading to apoptosis of the cell (12).

CTL induced apoptosis of HIV-1 infected cells is not however enough to eliminate the virus (12, 83). This is due to the virus's ability to escape CTL recognition through the development of escape mutations in epitopes (which may disrupt HLA-I binding or TCR recognition) or adjacent to viral epitopes (which may affect antigen presentation) (93). These viral variants undergo selective pressure that leads to CTL response driven HIV evolution (93) as the escape variants are deemed the most fit 'population' and their prevalence hence increases.

HIV-1 may also evade CTL responses through Nef-mediated selective HLA-I down-modulation (33, 91). Studies have shown that HIV-1 infected cells expressing Nef have reduced susceptibility to lysis by CTLs *in vitro*, and that in these cells HLA-I is internalised and ultimately degraded (91, 133). HLA-I (specifically HLA-A and HLA-B) down-modulation is initiated through the binding of Nef (EEEE motif, amino acids 62 – 65) with the phosphofurin acidic cluster-sorting signal 1 (PACS1) protein (134) (Table 1). PACS1 is detached when the

Nef/PACS1 complex localises to the *trans* golgi network (TGN) (134). Subsequently, Nef binds to a *src* family kinase (SFK) which in turn binds to and phosphorylates ZAP70/Syk on tyrosine (51, 64). ZAP70/Syk is phosphorylated in order to bind to the SH2 domain of phosphatidylinositide-3-kinase (PI3K) (51). PI3K activates ADP ribosylation factor 6 (ARF6) GTPase by triggering the transport of surface HLA-I to the TGN through the ARF6 compartment where it is ultimately degraded by accelerated HLA-A and -B endocytosis (64, 141).

1.6 Evidence for the role of Nef in HIV disease progression

The various activities of Nef which enhance HIV replication and contribute to evasion/subversion of immune responses as detailed above, suggests that Nef significantly enhances HIV pathogenesis. In this section, the evidence for the importance of Nef in HIV disease progression is discussed.

Progression to AIDS occurs on average within approximately 10 years of HIV-1 infection, however the time may differ significantly among individuals (81). Some individuals may progress to AIDS within 3 years or less of infection and are termed rapid progressors (143). On the other hand, a minority of HIV-1 infected people remain symptom free for prolonged periods (> 10 years in the absence of treatment) and may maintain stable levels of $CD4^+$ T cells in the normal or near-normal range (57). Such individuals are known as long-term non-progressors (LTNPs) (57, 81). An even lower number of HIV-1 infected individuals (< 1%) naturally suppress plasma viral loads to undetectable levels in the absence of treatment and are known as elite controllers (ECs) (123).

There is evidence that impairment of Nef function may contribute to slower disease progression in HIV infected individuals, as well as in SIV-infected macaques. Nef was shown to be an essential factor for the development of an AIDS-like disease in rhesus macaques and Nef-attenuated HIV strains have been isolated from LTNPs implicating Nef as a critical virulence factor for AIDS (81). Furthermore, Nef clones derived from ECs are functional but display significantly lower Nef-mediated activities (HLA-I and CD4 down-modulation, HLA-II invariant chain (CD74) up-modulation, viral infectivity enhancement and stimulated viral replication) compared to chronic progressors (123).

1.7 Treatment and preventive measures

1.7.1 Antiretroviral therapy (ART)

Since the introduction of combination antiretroviral therapy (cART) the number of AIDS related deaths has decreased (95). There are 25 antiretroviral (ARV) agents which constitute six categories of drugs that are licensed and available for the treatment of HIV-1 infection: seven nucleoside reverse transcriptase inhibitors (NRTIs), one nucleotide reverse transcriptase inhibitor (NtRTIs), four non-nucleoside reverse transcriptase inhibitors (NNRTIs), 10 protease inhibitors (PIs), cell entry inhibitors (one fusion inhibitor [FI] and one CC chemokine receptor 5 [CCR5] antagonist) and one integrase inhibitor (INIs) (34, 42, 144). Initial/first line therapy is based on a combination of two NRTIs and one potent agent from another drug class (148). Each component of a regimen is dependent on the specific situation of the individual who requires treatment (148).

Through the use of combination therapy plasma viremia is reduced thus increasing the life span of infected individuals, however the virus is not completely eliminated as the latent pool of HIV persists (34). Furthermore, ART is a life-long treatment, therefore there is a high risk for the development of drug resistance (34). In addition, a life time drug requirement results in a high cost factor. Even though life expectancy of HIV-1 infected people are increased with ART, the full life expectancy of these individuals remains diminished as these individuals have an increased risk of cardiovascular disease, metabolic disorders, neurocognitive abnormalities and frailty (95) to name a few.

Due to the limitations of ART outlined above, preventative measures are also required to fight the HIV epidemic. Examples of such preventative approaches in development include behavioural intervention (counselling), sexually transmitted infections (STIs) treatment, male circumcision and topical microbicides as pre/post-exposure prophylaxis (69). However, a HIV-1 vaccine would ultimately be the most cost effective and efficient way to control this global epidemic.

1.7.2 HIV vaccines

Despite the progress in understanding the interplay between HIV-1 and the human immune system, an effective vaccine against HIV-1 has not been developed (85). A successful vaccine has not been developed due to the major challenges in vaccine design (10, 85). Major challenges include the ability of the virus to integrate its genome into target cells as well as replicate and mutate rapidly: the rapid integration results in establishment of the viral latent reservoir which

narrows the window of opportunity where the virus could be eradicated by immune responses; while its rapid mutation rate enables the virus to evade human immune responses (116).

Thus far, there have been approximately 200 Phase I and II trials of vaccine candidates; more than 50 have gone to clinical human trial and only five Phase IIb and III efficacy trials have been performed (69, 112). The most recent Phase IIb and III trials have been the STEP study and the Thai trial (10, 69, 112). The vaccine group did not display a significant reduction in HIV-1 acquisition rates in any vaccine trials to date with the exception of the Thai trial (112) and no trials have shown slower disease progression in vaccinated individuals with break-through infections.

Briefly, the STEP trial tested a T cell based vaccine regimen containing an adenovirus serotype 5 (Ad5) vector and the HIV-1 clade B *gag*, *pol*, and *nef* genes (10). This vaccine was expected to better control viremia in individuals already exposed to the virus, rather than prevent new infections (10, 112). Even though the vaccine could elicit CTL responses, it failed to lower viral set-point (10, 112). The reason for lack of efficacy displayed by the vaccine remains unclear although it has been suggested that the failure may be associated with the range and specificity of CTL responses (112).

The Thai trial (RV144) on the other hand showed modest efficacy in protection from infection (69). In this trial, recombinant canarypox vector vaccine (ALVAC-HIV [vCP1521]) and

recombinant gp120 subunit vaccine booster injections (AIDSVAX B/E) was tested (137). This prime-boost vaccine resulted in 31% reduction in HIV incidence (69, 85) with $CD4^+$ T cell lymphoproliferation, antibody directed cell-mediated cytotoxicity (ADCC), antibodies binding to HIV-1 gp120 and neutralising antibody activities being the most common immune responses (112). However, a study showed that neutralising antibodies were only effective against several tier 1 viruses and not against tier 2 viruses (118). Therefore, the modest protection seen in the trial was attributed to alternate immune responses either acting alone or in combination with neutralising antibodies (69, 118). There is ongoing experimental testing of the RV144 vaccine to determine which component of the vaccine rendered it modestly effective (69). Even though 31 % efficacy is not sufficient, this trial shows that vaccine development is significantly closer since this is the first vaccine to partially block the acquisition of HIV-1 (112).

The ideal goal is to develop a vaccine that would prevent the establishment of HIV infection. It has been shown that several monoclonal antibodies (mAbs) have the capacity to neutralise a broad array of HIV-1 isolates and these have the potential to prevent HIV-1 infection, however, such antibodies have proven to be difficult to induce by vaccination, and the development of immunogens that elicit broadly reactive NAbs remains an important unsolved problem in HIV-1 vaccine development (10). Perhaps a more realistic goal might be a vaccine that does not completely eradicate the virus but suppresses viral load to low levels following infection and thereby slows disease progression (that is similar to EC or LTNP); such a vaccine could still have sufficient health impact (29). One such approach is to identify the most vulnerable regions of the virus and then target these with a vaccine immunogen, in order to limit immune escape or severely reduce fitness of the virus, thereby slowing disease progression (29).

1.8 Novel vaccine approach for rational immunogen design

1.8.1 Targeting vulnerable regions strategy: escape, fitness and disease progression

Fitness is a measure of an organism's adaptation to a given environment and is directly dependent on its ability to compete with other quasispecies (136). In a study which compared the fitness between a control group (expressing moderate *ex vivo* fitness), HIV-1 isolates from LTNPs and HIV-1 isolates from patients with accelerated progression to AIDS, LTNPs isolates were outcompeted by both the control as well as the accelerated progressor strains (136). As described previously (Section 1.6) Nef-attenuated strains results in slower progression to AIDS (81). Both studies provide evidence that viral fitness is a factor which significantly contributes to HIV-1 disease progression. Furthermore, several studies have shown that viral escape mutations within highly conserved Gag capsid protein epitopes and which are also associated with protective HLA alleles significantly reduce viral replicative capacity (17, 39, 109). Troyer *et al*. (2009) also show that mutations in highly conserved regions are more likely to result in a viral fitness cost than those in more variable regions (149).

Therefore, continuous immune pressure on the wild-type virus favouring the outgrowth of escape variants with diminished fitness is a suggested vaccine strategy (7, 29). Although promising, this strategy poses a challenge because HIV-1 develops compensatory mutations that restore or partially restore its reduced fitness (17, 29, 39). Recently, computational models have been designed that attempt to address these challenges, a discussion of which follows.

1.8.2 Computational models

1.8.2.1 Sectors

A study by Dahirel *et. al* (2007) sought to address the challenge of immune escape and ease of compensation for loss of fitness, by identifying higher order constraints on the development of HIV mutations (40). They developed a computational model using statistical physics to identify groups of co-evolving amino acids in the HIV Gag protein that evolved independently from other groups and termed such groups 'sectors' (40). Five Gag sectors were identified and correlations between multiple mutations at sites that comprise each collectively evolving sector were determined (40). A negative correlation between sites implies that the simultaneous mutations at these sites are observed less frequently (and therefore expected to result in less fit virus) than if the individual mutations were to arise independently (40). Thus, it is expected that the greater the proportion of negative correlations in a sector, the more difficult it would be for the virus to escape the CTL pressure and maintain virus fitness should multiple sites within the sector be targeted by CTLs (leading to maintained immune pressure) (40). Such an immunologically vulnerable sector (termed sector 3) was identified in which escape and compensatory pathways are expected to be restricted and supporting these hypotheses, elite controllers preferentially target this sector (40).

1.8.2.2 Fitness landscape

However, the sector model does not provide information about the fitness of strains with specific mutations in combination and cannot identify viable escape pathways that remain after targeting the vulnerable sector (49). This model was therefore extended by the development of a model

that can predict fitness landscape of any viral strain as a function of its amino acid sequence (49). Multiple sequence alignments (MSA, biological alignment of subtype B sequences) extracted from infected hosts, captured in the Los Alamos National Laboratory HIV Database [http://www.hiv.lanl.gov], were downloaded, processed and then used to generate the model. The model is based on the Ising spin glass model from statistical physics (49). The presence of mutations or the wild-type amino acid at each codon within each sequence in the MSA was defined using a binary approximation. The wild-type amino acid was denoted by zero and a mutant amino acid was denoted by one. This code therefore does not consider the identity of the mutant amino acid, however it is a good approximation for highly conserved proteins.

The model assigns an 'energy' (E) value to each viral strain. This E value is related to the probability of observation of the strain within the population and is predicted to be inversely related to replicative fitness (49). The model thus provides comprehensive information on viral fitness landscape and may potentially be used to predict replicative fitness of various mutant strains, viable escape pathways that remain after targeting vulnerable regions and how to restrict viable immune escape, hence serving as a potential tool for HIV-1 immunogen design (49). The model however, requires validation with *in vitro* experiments and experiments using animal models (49).

Thus far, the fitness landscape model for the highly conserved Gag protein as been tested (49). For the *in vitro* experiments, 19 different mutations (16 single and 3 paired mutations) in Gag p24 were introduced in HIV-1 clade B NL4-3 backbone (49). The replication capacity of each

mutant was measured and plotted against the energies of the same mutants predicted by the model (49). A strong negative correlation was observed between the two plotted variables which showed that the *in vitro* data supported model predictions (49).

More recently, the fitness landscape model for Gag was computationally advanced and further tested by measuring the *in vitro* replication capacities of HIV strains containing multiple mutations – 43 different mutants were tested in total (105). As previously, *in vitro* data correlated well with model predictions. Model advancements included the introduction of Bayesian regularisation: previously, strains containing pairs of mutations not present in the MSA database were inferred as having a zero probability. However, this may have been due to a limitation of the sample size, which is corrected for in newer models by Bayesian regularisation. The resulting regularised model predicts non-zero values for sequences containing mutations not observed in the sequence database. Further, an advanced modelling approach, the Potts model, was developed to address a major drawback of the Ising model: it cannot predict the fitness differences between strains containing different mutations at a particular position. This may in particular pose a disadvantage for predicting the fitness consequences of mutations in highly variable proteins such as Env and Nef. The Potts model takes specific amino acid mutations into account rather than using the binary approximation (as detailed above).

1.9 The present study

Despite the growing epidemic and research efforts there still exists limitations of ART and a vaccine against HIV-1 remains elusive, mainly due to high mutability of the virus and its

consequent immune evasion (Section 1.7). Computational models predicting the viral fitness landscape are a novel and promising approach to rational, rather than empirical, vaccine design that have the potential to overcome the challenge of HIV-1 immune evasion (Section 1.8). These models however require validation by *in vitro* and animal model experimental procedure (Section 1.8). As mentioned previously, the fitness landscape model for the highly conserved Gag protein has been tested, and the *in vitro* data strongly supports the fitness model predictions (Section 1.8). In such a highly conserved protein, escape mutations would likely result in a fitness cost to the virus, however, it is not expected that mutations in variable proteins such as Nef would result in a fitness cost (Section 1.8). However, Nef may be a desirable vaccine target since it plays an essential role in increasing HIV virulence and pathogenicity and enhancing viral replication (Sections 1.4 - 1.6). Furthermore, Nef is highly immunogenic with many HLA-associated mutations potentially conferring escape from CTL responses (19). Nef was included in the unsuccessful STEP trial vaccine (21), however there is little evidence for or against its inclusion in vaccine strategies.

The fitness landscape model of Nef has not yet been tested, but could potentially reveal vulnerable regions of Nef and indicate suitability for inclusion of specific Nef epitopes in a vaccine. The present study is in collaboration with the developers of the fitness landscape model. Collaborators have applied modelling approaches to the Nef protein, and the present study will test various combinations of mutations in Nef (spanning a wide range of predicted E values) predicted to be either harmful or not harmful to HIV-1 replication. The performance of the Potts and Ising models for Nef will be compared to determine whether the Potts model can better predict the effect of different combinations of mutations in the highly variable HIV-1 Nef protein

than the Ising model, as is expected to be the case (Section 1.8.2.2). We will measure the fitness of the various Nef mutants in peripheral blood mononuclear cells (PBMCs) as previously described (123) because the presence of Nef is not essential for viral replication in many immortalised T cell lines (100). In addition to measured viral fitness, two well-described and pathogenic functions of Nef: CD4 down-modulation (which enhances HIV-1 infectivity and replication) and HLA-I down-modulation (which enhances immune evasion) (51) will be measured, since HLA down-modulation potentially does not directly influence HIV replication *in vitro*, yet may still play a significant role in HIV-1 pathogenesis. Specific aims and objectives of the present study are outlined below.

1.9.1 Aim

To evaluate and compare the accuracy of the Ising and Potts models in predicting the fitness consequences of mutations in HIV-1 Nef through directly testing *in vitro* the effect of various mutations and mutation combinations on HIV-1 replication ability and Nef functions.

1.9.2 Objectives

- Introduce combinations of mutations into the consensus B *nef* gene, cloned into an HIV-1 NL4-3 plasmid, by site directed mutagenesis and confirm the presence of mutations by sequencing.
- Generate stocks of mutant viruses by electroporation of a green fluorescent protein (GFP)-reporter T cell line with mutant plasmids.
- Assay *in vitro* replication capacities of mutant viruses in PBMCs using ELISA.

- Clone the mutant *nef* sequences into a GFP-expressing plasmid, transfect cells with clones and measure cell-surface expression of CD4 and HLA-I in transfected cells by flow cytometry to determine the Nef-mediated CD4 and HLA-I down-modulation capacities of the mutant viruses.

CHAPTER 2

MATERIALS AND METHODS

2.1 Ethical considerations

The proposed study was approved as and forms part of a study protocol (Investigation of the viral fitness landscape in and around multi-dimensionally conserved regions of HIV-1) for which ethical approval has been obtained from the Biomedical Ethics Research Committee of the Nelson R Mandela School of Medicine (University of KwaZulu-Natal) (Ref: BE166/11).

2.2 Mutation selection

To evaluate and compare the ability of the Ising and the Potts models in predicting the fitness consequences of mutations in HIV-1 Nef, by *in vitro* experimental procedures, several mutations and mutation combinations were selected for testing based on their predicted energies. As mentioned previously, the models assign an energy (E) value to each viral strain which is predicted to be inversely related to the replicative fitness of the strain (49).

Mutants were selected so that they covered a range of E values. We included mutations in known functional motifs involved in CD4 and HLA down-modulation for comparison to what has been documented in literature. We also included HLA-associated mutations (likely to be CTL escape mutations) or known CTL escape mutations that covered a range of E values, since it would be desirable to identify CTL escape mutations with functional costs. Mutations with differential E at the same codon were also chosen to test the ability of the Potts model to distinguish between and account for different substitutions at the same codon. All mutations, as well as their E values predicted by the Ising and Potts models and the reasons for their selection are summarised in Table 2.1.

Table 2.1. Energies, predicted by the Ising and Potts models, of the selected mutants

Category	Mutant[a]	Ising E[a]	Potts E[b]	
				Previously shown to be required for down modulation of:
Known functional motifs	17K19K	10.15	10.60	HLA and to a lesser extent CD4 (141)
	57G	6.60	6.73	CD4 (60, 67, 104)
	57R	6.60	5.16	CD4 (60, 67, 104)
	57R58P	10.70	9.67	CD4 (60, 67, 104)
	72L75L	12.85	13.92	HLA (52, 104)
	123G	5.95	7.48	HLA and CD4 (52, 60)
				Associated with HLA-[c]
HLA associated/ known CTL escape mutants/ Mutant--pairs	28E	-0.20	1.43	C*08:02
	33A	1.11	1.89	A*68:01. 33V known escape mutant (62)
	43L	1.45	4.16	43V associated with C*03
	71K	1.60	1.48	C*07:02 and 71T with B*07:02. 71T and 71R are known escape mutants (98, 122, 150)
	76V	3.72	4.95	B*81 and C*18:01. 76V, 76T, 76I are known escape mutants (92)
	80D	3.74	6.07	B*35:01 and C*07:02
	80N	3.74	4.52	B*07:02
	88G	3	8.94	Known escape mutant (28)
	102H	-0.60	0.98	B*44:03 and C*08
	102W	-0.60	4.28	
	133T	-0.97	0.8	B*35:01, 133I with B*38:01 and B*57
	135F	0.92	2.23	A*23:01 and A*24. A known escape mutant (56)
	143Y	3.57	2.88	A*23:01
	188H	1.55	2.72	A*31:01, 188R with B*58:01 and 188S with A*30:01. 188N known escape mutant (62)
	192R	0.99	2.47	192K associated with A*74. A known escape mutant (77)
	28E102H	0.43	2.60	
	28E102W	0.43	6.10	
	33A43L	1.47	2.87	
	43L88G	5.40	13.29	
	71K76V	6.53	6.57	
	76V80N	8.16	9.62	
	133T135F	-1.22	0.58	
	135F143Y	7.56	6.28	
	188H192R	1.74	2.61	
Variable amino acids at same codon	21E	-0.34	5.31	Chosen to test the ability of the Potts model to distinguish between, and assign E values accordingly, for different mutations at the same codon
	21K	-0.34	0.58	
	57G[d]	6.60	6.73	
	57R[d]	6.60	5.16	
	80D[d]	3.74	6.07	
	80N[d]	3.74	4.52	
	102H[d]	-0.60	0.98	
	102W[d]	-0.60	4.28	
	28E102H	0.43	2.60	
	28E102W	0.43	6.10	

[a]All mutants chosen represent the most common mutation at the corresponding residue with the exception of the additional mutations chosen to test the ability of the Potts model to distinguish between different amino acids at the same codon

[b]The energies were computed for the mutations in the consensus B sequence background, where any sequence differences from the MSA consensus sequence were considered as additional mutations

[c]Lists of HLA-associated polymorphisms in Nef were derived from (22, 23)

[d] Mutants repeatedly listed in the table i.e. mutants which fall into more than one category

2.3 Preparation of the LANL consensus B *nef* NL4-3 plasmid

The mutations listed in Table 2.1 were introduced into the consensus B *nef* sequence (2004 consensus sequence available from the Los Alamos Sequence database [LANL]), kindly donated by Dr. Mark Brockman (Simon Fraser University, Canada, formerly of the Ragon Institute of Massachusetts General Hospital, Massachusetts Institute of Technology and Harvard University). The LANL consensus B *nef* sequence was chosen since it differed by only nine amino acids from the Nef MSA (multiple sequence alignment) consensus sequence. The LANL consensus B *nef* sequence was provided in the background of the pselect plasmid (Invivogen, San Diego, USA). Prior to performing site-directed mutagenesis, this LANL consensus B *nef* sequence was cloned into an ampicillin-resistant HIV-1 subtype B NL4-3 plasmid using restriction enzymes. A modified NL4-3 plasmid containing NcoI and NotI restriction enzyme sites on either side of the *nef* gene, respectively, was kindly donated by Dr. Takamasa Ueno (Kumamoto AIDS Research Centre, Kumamoto, Japan). The cloning of LANL consensus B *nef* into NL4-3 is described below and illustrated in Figure 2.1.

2.3.1 PCR amplification of LANL consensus B *nef* to introduce NcoI and NotI restriction sites

A 50 µl PCR reaction was performed to introduce NcoI and NotI sites on either side of the LANL consensus B *nef* gene using the Expand High Fidelity PCR System (Roche Applied Science, Mannheim, Germany).

Figure 2.1. Cloning LANL consensus B *nef* into NL4-3

The LANL consensus B *nef* sequence was amplified by PCR from the LANL consensus B *nef* pselect plasmid and both the amplified product as well as the NL4-3 plasmid were digested with NcoI and NotI enzymes. The products were then ligated using T4 DNA ligase and transformed into *E. coli* cells. The transformed cells were then plated on LB agar plates which contained ampicillin to select for cells transformed with the ampicillin-resistant NL4-3 plasmid. The presence of the LANL consensus B *nef* sequence was confirmed by sequencing and a colony that contained this sequence was purified by a maxiprep procedure.

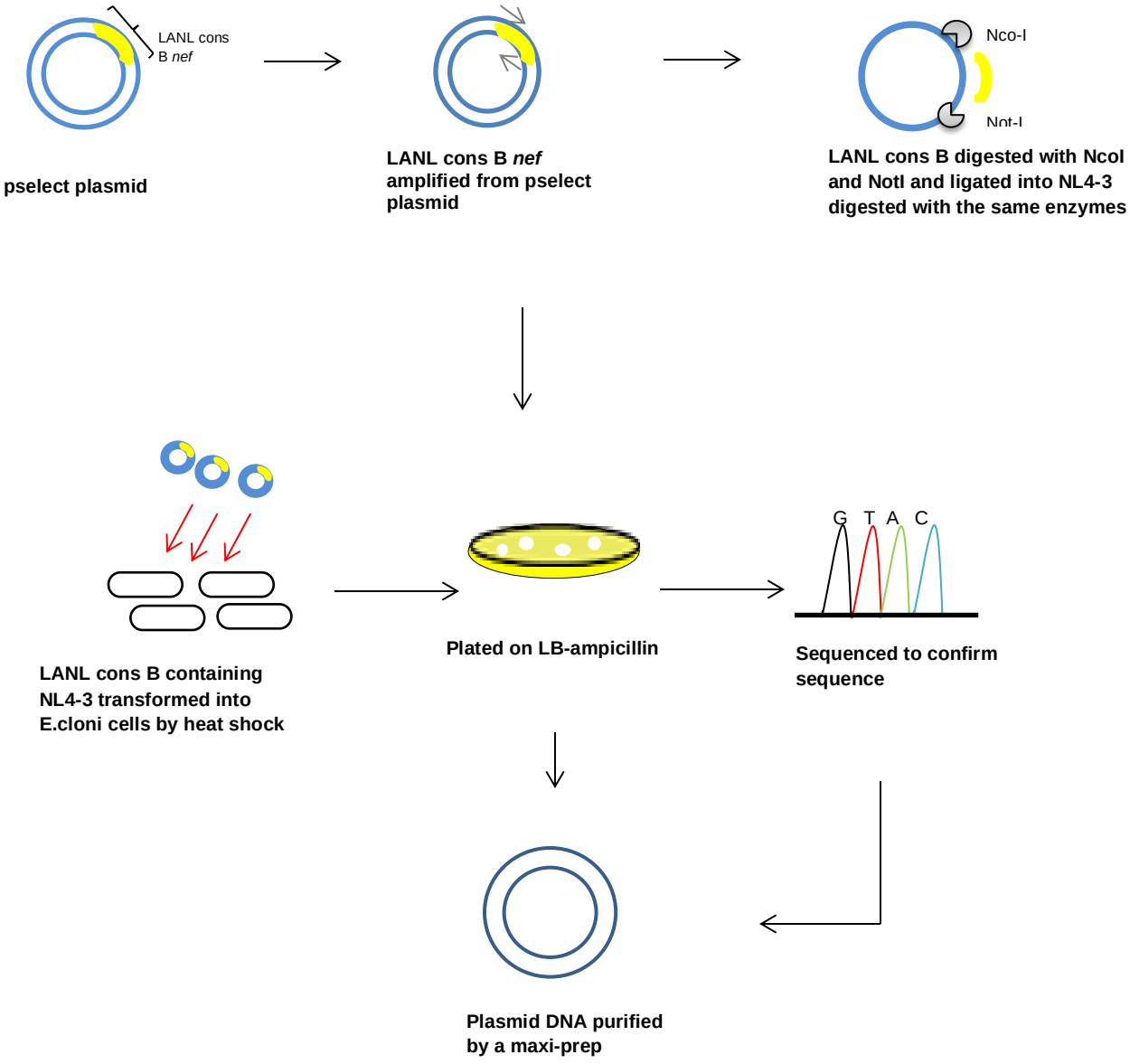

pselect plasmid

LANL cons B *nef* amplified from pselect plasmid

LANL cons B digested with NcoI and NotI and ligated into NL4-3 digested with the same enzymes

LANL cons B containing NL4-3 transformed into E.cloni cells by heat shock

Plated on LB-ampicillin

Sequenced to confirm sequence

Plasmid DNA purified by a maxi-prep

The reaction comprised 0.75 µl Roche enzyme, 5 µl Buffer 2, 2 µl Buffer 4, 4 µl of 2.5 mM deoxyribonucleotide triphosphate (dNTPs, TaKaRa Ex Taq HS enzyme kit [Takara, Shiga, Japan]), 1 µl of 10 µM forward primer (5' CTTTGAARCAGCTTTGCTATAAA**CCATGG**G 3', NcoI site in bold), 1 µl of 10µM reverse primer (5' AAAGTCCCAGGCGGAAAGTCC **GCGGCCGC**TCAGCAG 3', NotI site in bold), and 2 µl of 25 ng/µl LANL consensus B *nef* pselect plasmid. The PCR was run on a thermocycler with an initial denaturation at 94 °C for 2 minutes, 35 cycles of denaturation at 94 °C for 15 seconds, annealing at 55 °C for 30 seconds, extension at 72 °C for 2 minutes with a 5 second increment after every cycle; and a final extension step at 72 °C for 7 minutes. 5 µl of the PCR product was mixed with 2 µl loading dye containing GelRed, electrophoresed on an agarose gel (1 % [weight of agarose to volume of buffer]) using Tris Borate EDTA (TBE) buffer and visualised using a G:BOX. The remainder of the product was purified using the QIAquick PCR purification kit (Qiagen, Valencia, USA) according to the manufacturer's protocol.

2.3.2 Digestion of LANL consensus B *nef* PCR product and modified NL4-3 plasmid containing NcoI and NotI sites

Purified LANL consensus B *nef* PCR product (5 µg) and NL4-3 plasmid (5 µg) were both digested with restriction enzymes NotI (10 U) and NcoI (10U) (New England Biolabs, Hitchin, UK) in the presence of Buffer 3.1 (1 ×) and water (to a final volume of 50 µl). The reaction was incubated at 37 °C for 1 hour and the enzyme inactivated at 65 °C for 20 minutes. Digested products were electrophoresed in the presence of Tris Acetate EDTA (TAE) buffer. The digested products were then excised from the gel (avoiding exposure to UV light, as this degrades DNA)

and purified using the GeneJET Gel Extraction Kit (Thermo Scientific) according to the manufacturer's protocol.

2.3.3 Ligation of digested LANL consensus B *nef* and NL4-3

Gel purified digested LANL consensus B (30 ng) and NL4-3 (186 ng) were ligated using 3U of T4 DNA ligase (Promega, Madison, USA) in a final reaction volume of 20 µl. The reaction was incubated at 22 °C overnight, followed by an inactivation of the enzyme at 65 °C for 10 minutes. 1 µl ligation product was transformed by heat shock into 33 µl E.cloni cells (Lucigen, Middleton, USA) and plated on Luria-Bertani (LB) ampicillin agar plates (100 µg ampicillin per 1 ml broth), according to manufacturer's instructions.

2.3.4 Verification of the LANL consensus B *nef* NL4-3 clone by colony PCR and sequencing

2.3.4.1 Colony PCR

PCR, followed by gel electrophoresis, was used to determine the presence of *nef*-containing plasmid in colonies as follows: colonies were picked from the transformation plate, touched on another LB-ampicillin agar plate to keep a record of the colonies, and dissolved in 10 µl PCR water. This suspension was briefly vortexed and boiled in a thermocycler at 98 °C for 10 minutes. The 10 µl PCR reaction was performed using the TaKaRa Ex Taq HS enzyme kit (Takara, Shiga, Japan) and utilised 6.6 µl PCR water (Bioline, Taunton, USA), 0.08 µl Ex Taq DNA polymerase, 0.8 µl dNTPs, 1 µl Ex Taq buffer, 0.25 µl each of 10 µM Nef-specific primers (forward primer: 5' ACATACCTASAAGAATAAGACAGG 3', and reverse primer: 5'

GTCCCCAGCGGAAAGTCCCTTGT 3'), and 1 µl boiled colony. The PCR was run for 35 cycles: denaturation at 94 °C for 15 seconds, annealing at 55 °C for 30 seconds and extension at 72 °C for 1 minute and 30 seconds with an initial denaturation at 94 °C for 2 minutes and a final extension step at 72 °C for 7 minutes. The *nef*-containing colonies were then sequenced to verify the LANL consensus B *nef* sequence.

2.3.4.2 Sequencing of the colony PCR product

Sequencing was performed using the ABI Prism Big Dye Termination V 3.1 cycling sequencing kit (Applied Biosystems, Foster City, USA) in a 96-well plate (Applied Biosystems). Each 10 µl reaction comprised 4 µl PCR water (Bioline), 2 µl sequencing buffer, 0.4 µl BigDye mix, 2.6 µl Nef-specific primer: 5' GTGGAAAGTCCCAGGCGGAAAG 3' (2 µM) and 1 µl diluted template DNA (1 µl colony PCR product diluted in 14 µl PCR water [Bioline]). The following cycling conditions were used: initial denaturation at 96 °C for 1 minute with 25 cycles of denaturation at 96 °C for 10 seconds, annealing at 50 °C for 5 seconds and extension at 60 °C for 4 minutes. A sequencing plate clean-up was then performed on the fresh sequencing products. 1 µl of 125 mM ethylenediaminetetraacetic acid (EDTA) plus a mix of 1 µl sodium acetate at 3 M with 1 µl absolute ethanol were added to each product. The plate was then covered with foil and the reactions were mixed by vortex for 5 seconds which was followed by centrifugation at 3000 rpm for 20 minutes. The supernatant was removed by inverting the plate on tissue paper and centrifuging at 180 rpm for 1 minute. The pellets were washed with 35 µl ethanol (70 %) and centrifuged at 3000 rpm for 5 minutes. Again, the supernatant was removed by inverting the plate on tissue paper and centrifugation at 180 rpm for 1 minute. The products were then dried in a thermocycler at 50 °C for 5 minutes and stored at - 20 °C until further use.

These products were re-suspended in 10 µl formamide and vortexed. The plate was then incubated in a thermocycler at 95 °C for 3 minutes and at 4 °C for 3 minutes. The sequences were then compiled using the ABI 3130xl Genetic Analyzer (Applied Biosystems). Sequences were compared to the LANL consensus B *nef* sequence using Sequencher 5.0 (Gene Codes Corporation, Ann Arbor, USA).

The colony verified to contain the correct LANL consensus B *nef* sequence was then inoculated into 3 ml LB-ampicillin broth (100µg ampicillin per 1 ml broth) followed by incubation at 37 °C and 250 rpm for 2 hours. This culture was then used to inoculate 100 ml of fresh LB-ampicillin broth, at the same concentration, which was incubated overnight at 37 °C and 250 rpm. The LANL consensus B *nef* NL4-3 plasmid was then purified from these bacterial cells by a maxi-prep procedure (Qiagen) according to manufacturer's instructions.

2.4 Site-directed mutagenesis of the LANL consensus B *nef* NL4-3 plasmid

Mutations (Table 2.2) were introduced into the LANL consensus B *nef* NL4-3 plasmid using the QuikChange II XL Site-Directed Mutagenesis kit (Stratagene, La Jolla, CA) according to manufacturer's indications. Briefly the procedure involved the generation of mutants (containing staggered nicks) through PCR amplification of the desired template with mutagenic primers, listed in Table 2.2. This was followed by selective removal of the original unmutated plasmid by digestion of the PCR product with DpnI, which specifically recognises and cleaves methylated DNA that is present only in the original plasmid. The nicked mutant plasmid was then transformed into XL10-Gold Ultracompetent cells for nick repair.

Table 2.2. Primers used in site-directed mutagenesis to induce the desired mutations

Mutant[a]	Primer sequence[b]
17K19K	GGATGGCCTACTGTAAAGGAAAAAATGAGACGAGCTGAGCC
21E	CCTACTGTAAGGGAAAGAATGGAACGAGCTGAGCCAGCAGCAG
21K	CCTACTGTAAGGGAAAGAATGAAACGAGCTGAGCCAGCAGCAG
28E	CGAGCTGAGCCAGCAGCAGAAGGGGTGGGAGCAGTATC
33A	GCAGATGGGGTGGGAGCAGCATCTCGAGACCTGGAAAAAC
43L	CCTGGAAAAACATGGAGCACTCACAAGTAGCAATACAGCAGC
57G	GCTAACAATGCTGATTGTGCCGGGCTAGAAGCACAAGAGGAGG
57R	GCTAACAATGCTGATTGTGCCCGGCTAGAAGCACAAGAGGAGG
57R58P	GCTGATTGTGCCCGGCCAGAAGCACAAGAGG
71K	GGAGGAGGAGGTGGGTTTTCCAGTCAAACCTCAGGTACCT
72L75L	GGGTTTTCCAGTCAGACTTCAGGTACTTTTAAGACCAATGAC
76V	CCTCAGGTACCTGTAAGACCAATGACTTACAAGGG
80N	CAGGTACCTTTAAGACCAATGAATTACAAGGGAGCTTTAGATC
76V80N	GACCTCAGGTACCTGTAAGACCAATGAATTACAAGGG
80D	CAGGTACCTTTAAGACCAATGGATTACAAGGGAGCTTTAGATC
88G	CAAGGGAGCTTTAGATCTTGGCCACTTTTTAAAAGAAAAGGGGGG
102H	GGGGGGACTGGAAGGGCTAATTCACTCCCAAAAAAGACAAG
102W	GGGGGGACTGGAAGGGCTAATTTGGTCCCAAAAAAGACAAG
123G	CACACAAGGCTACTTCCCTGGATGGCAGAACTACACACCAGGG
133T	CACACCAGGGCCAGGGACCAGATATCCACTGACCTTTGG
135F	CCAGGGCCAGGGATCAGATTTTCCACTGACCTTTGGATGG
133T135F	CACACCAGGGCCAGGGACCAGATTTTCCACTGACCTTTGGAT
143Y	CCACTGACCTTTGGATGGTGCTACAAGCTAGTACCAGTTGAGCC
188H	GTGTGGAAGTTTGACAGCCACCTAGCATTTCATCACATGGCC
192R	GACAGCCGCCTAGCATTTCGTCACATGGCCCGAGAGC
188H192R	GTTTGACAGCCACCTAGCATTTCGTCACATGGCCCGAGAGC

[a]In order to create the mutation combinations 28E102H, 28E102W, 33A43L, 43L88G, 71K76V and 135F143Y, independent primers were not utilised, instead primers designed to create the single mutants were used in combination in the site-directed mutagenesis reaction as these primers did not overlap with each other.

[b]The table contains the forward primer sequences (5' – 3' direction) and the reverse primer sequences are the reverse complements of the forward primers. The mutated codon in each primer is underlined and the nucleotide change is highlighted.

To determine transformation success, a PCR was performed on colonies as described in Section 2.3.4.1. In addition, sequencing (described in Section 2.3.4.2) was performed to confirm the presence of the correct mutation in *nef*-containing colonies. Plasmid DNA was then purified from the colonies confirmed to contain the correct mutant sequence by the Qiagen maxi-prep procedure. The site-directed mutagenesis procedure is depicted in Figure 2.2.

Since the HIV-1 Nef sequence partially overlaps with the 3' LTR sequence (Figure 2.3), the primers for mutations in the overlapping region after codon 96 will bind to both the Nef sequence and the 5' LTR sequence present in the LANL consensus B *nef* NL4-3 plasmid. Therefore, for these specific mutations, the LANL consensus B Nef sequence was cloned into the TOPO vector using the TOPO TA Cloning kit pCR 2.1 (Invitrogen, Carlsbad, USA) prior to mutagenesis. Following confirmation of the presence of the correct mutations, the mutated Nef sequence was cloned back into NL4-3 as described in Section 2.3.

2.5 Generation of mutant virus stocks

In order to generate the mutant viruses, a CEM-derived T cell line, CEM-GXR25 (GXR; donated by Dr. Mark Brockman) was transfected with the mutant plasmids, as described previously (160) and briefly in Section 2.5.2. These $CXCR4^+$ and $CCR5^+$ GXR cells encode GFP which is Tat-dependent and driven by HIV-1 LTR. GFP is produced following HIV-1 infection which allows for the detection of infected cells by flow cytometry (18). This procedure is demonstrated in Figure 2.4.

Figure 2.2. Site-directed mutagenesis

The NL4-3 plasmid was PCR amplified with mutagenic primers to induce the desired mutations, followed by digestion with DpnI to selectively remove the original plasmid since this enzyme specifically recognises and cleaves methylated DNA present in the original, yet not the modified, plasmid. Following mutagenesis, plasmids were transformed by heat shock into competent bacterial cells which were then plated on LB-ampicillin agar plates to allow for specific reproduction of the cells transformed with the ampicillin-resistant plasmid. Plasmid DNA was purified from the bacterial cells by a maxi-prep procedure and the presence of the desired mutations confirmed by sequencing.

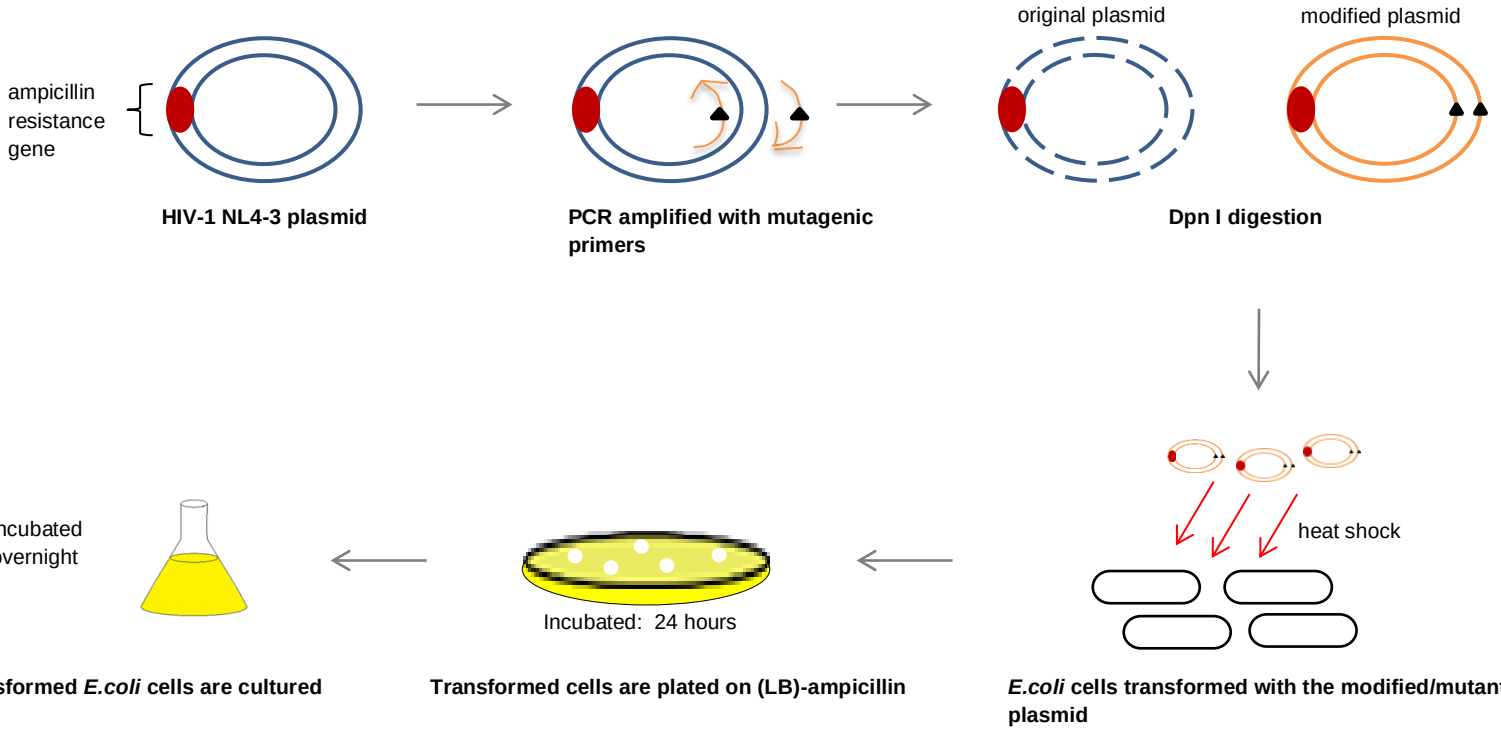

HIV-1 NL4-3 plasmid

PCR amplified with mutagenic primers

Dpn I digestion

***E.coli* cells transformed with the modified/mutant plasmid**

Transformed cells are plated on (LB)-ampicillin

Transformed *E.coli* cells are cultured

Plasmid DNA purified by a maxi-prep procedure

Plasmid DNA sequenced to confirm the presence of mutations

Figure 2.3. HIV-1 genome organization (from http://www.hiv.lanl.gov/) (1)

HIV-1 genes and gene products are represented as rectangles and are numbered relative to HIV-1 HXB2. In addition, the DNA sequence flanking the genome (Long terminal repeat (LTR) region) is depicted. HIV-1 Nef overlaps with the 3' LTR region from codon 96 to codon 206.

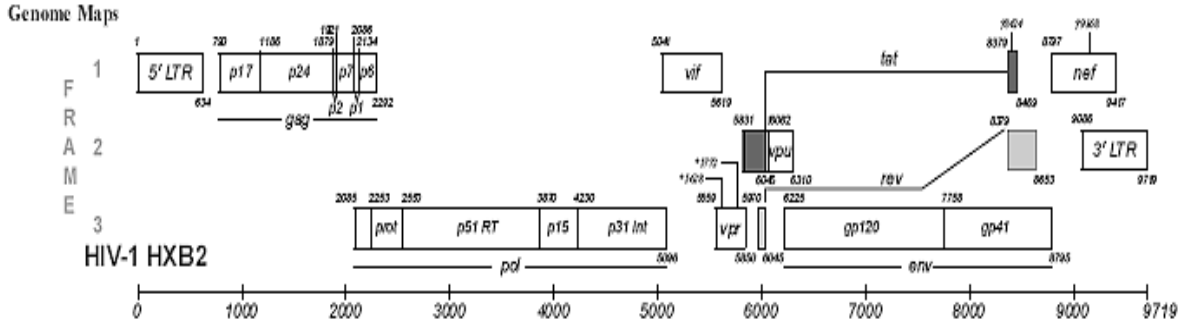
Genome Maps
FRAME
1
2
3
5' LTR
p17
p24
p7
p6
p2
p1
gag
vif
tat
rev
nef
vpu
3' LTR
TRV
prot
p51 RT
p15
p31 Int
pol
vpr
gp120
gp41
env
HIV-1 HXB2
0
1000
2000
3000
4000
5000
6000
7000
8000
9000
9719

Figure 2.4. Generation of virus stocks from mutant plasmids

GXR cells were transfected with the mutant plasmids via electroporation at 250 V and 950 µF. The cells were maintained in R10 medium and incubated at 37 ℃ and 5 % CO_2. Virus growth was monitored by flow cytometry and when approximately 30 % of the cells were infected, the culture was centrifuged at 4 ℃ and 1700 rpm for 5 minutes. The viral supernatant was aliquoted and stored at – 80 ℃ until further use in virus titration and replication capacity assays.

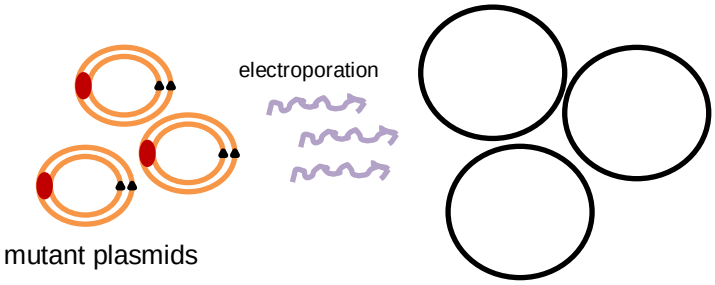

GXR cells transfected with mutant plasmid via electroporation

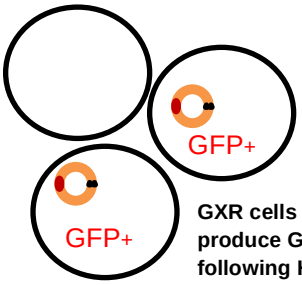

GXR cells produce GFP following HIV-1 infection

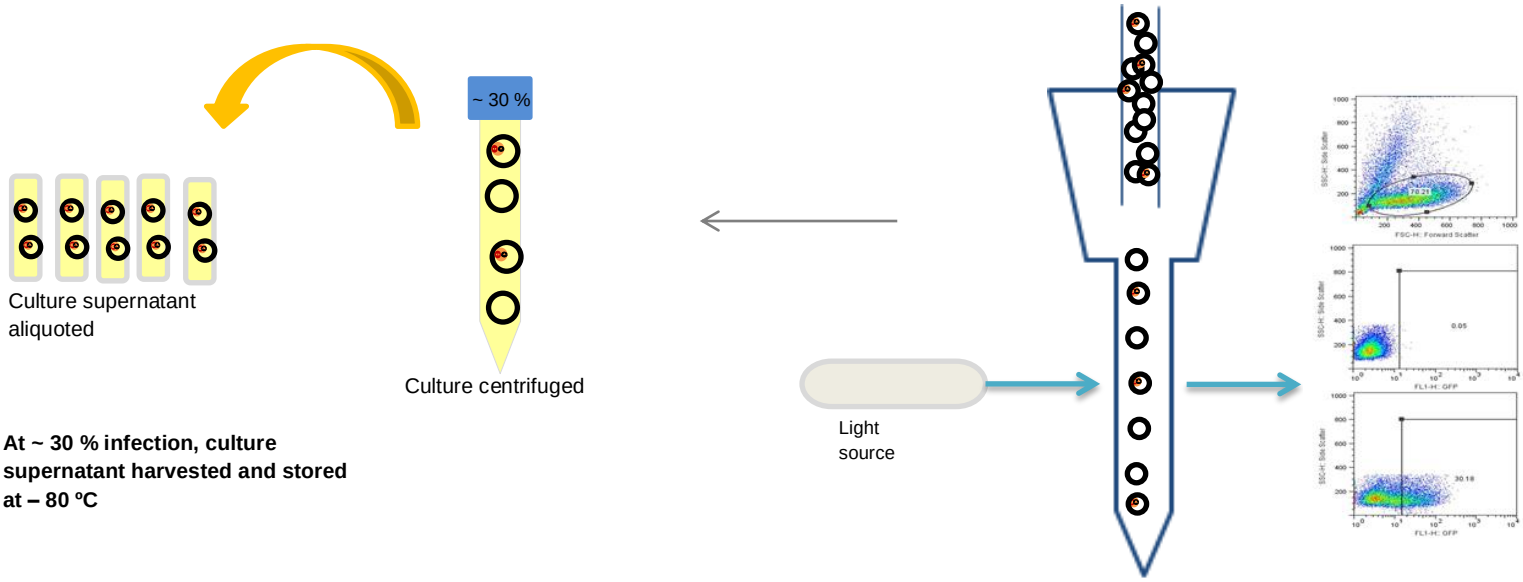

At ~ 30 % infection, culture supernatant harvested and stored at – 80 ºC

% of infected GXR cells measured every 2 days by flow cytometry

2.5.1. Culturing of GXR cells

GXR cells were stored in a liquid nitrogen freezer (Custom Biogenics Systems, Romeo, USA) at 5 million cells in 1ml R10 medium (RPMI-1640 [Sigma, St Louis, USA] supplemented with 10% foetal bovine serum (FBS) [Gibco, New York, USA], 2 mM L-glutamine [Sigma], 10 mM N-2-hydroxyethylpiperazine-N'-2-ethanesulfonic acid (HEPES) [Gibco], and 50 U per ml penicillin-streptomycin [Gibco]) containing 10 % dimethylsulfoxide (DMSO). Frozen GXR cells were thawed in a water bath at 37 ℃. The thawed aliquot was then added into a T25 flask (Corning-Costar, New York, USA) containing 4 ml pre-warmed R10 medium and incubated at 37 °C and 5 % CO_2. The following day, to remove DMSO, the 5 ml cell culture was centrifuged at 1500 rpm for 10 minutes and the supernatant discarded. The pelleted cells were then re-suspended in 10 ml pre-warmed R10 medium and again incubated at 37 ℃ and 5% CO_2. Once cells had recovered and proliferated (as indicated by a change in colour of the R10 medium from red to yellow, due to the presence of phenol red indicator in the medium), the GXR stock culture was thereafter maintained in a T75 flask (Corning-Costar).

2.5.2 Transfection of GXR cells with mutant plasmids

The number of cells present in the GXR stock culture was counted using the TC10 automated cell counter (Biorad, Hercules, USA). Briefly, 10 µl of the stock culture was mixed with 10 µl of trypan blue (0.4 %) and 10 µl of the mixture added into the chamber of the disposable slide (Biorad), which was then inserted into the cell counter. The trypan blue allows distinction between live and dead cells. The required number of live GXR cells (five million cells per sample: four million electroporated and one million unelectroporated) were pelleted by

centrifugation at 1500 rpm for 10 minutes. The four million cells (per sample) that were pelleted for electroporation were re-suspended in 300 µl R10 medium and transferred to a 0.4 cm electroporation cuvette (Biorad), while the 1 million cells (per sample) that were not to be electroporated were re-suspended in 1ml R10 medium supplemented with 4 µl of polybrene (10 mg/ml, Millipore) and added to 9 ml R10 medium in a T25 flask. Each mutant plasmid (10 µg, Section 2.5.) was added to the 4 million GXR cells in the electroporation cuvette and mixed by pipette. This mixture was subjected to electroporation in a Gene Pulser II (Biorad) at 250 V and 950 µF. The electroporated cells were rested for 5 minutes and transferred into the T25 flask containing the non-electroporated cells. Five days after transfection, 5 ml R10 medium was added to each flask, and virus growth was thereafter monitored by flow cytometry as described next.

2.5.3 Measurement of virus growth by flow cytometry

Six days after transfection, 1 ml of the cell culture was removed (followed by replacement with fresh R10 medium) and pelleted by centrifugation at 1500 rpm for 10 minutes in a cluster tube (Corning). The supernatant was discarded and the tubes vortexed to re-suspend the cell pellet in the remaining supernatant. The cells were fixed with 200 µl of 2% paraformaldehyde (PFA). These cells were then measured for GFP expression by flow cytometry on a FACSCalibur (BD Biosciences, San Jose, USA) to determine the percentage of infected cells (GFP-positive cells). The culture was monitored every 2 days until harvesting.

2.5.4 Harvesting virus stocks

When approximately 30 % of the cells were infected, the culture supernatant was harvested. This was done by centrifuging the culture at 4 °C and 1700 rpm for 5 minutes and storing 1 ml aliquots of the virus containing supernatant at – 80 °C.

2.6 Titration

The virus stocks were diluted 4000 × in R10 medium and levels of p24 in these viruses were quantified by ELISA using the Retro-trek HIV-1 p24 Antigen ELISA 2.0 kit (ZeptoMetrix corporation, New York, USA) according to manufacturer's indications. All wash steps were performed using the ELx50 auto strip washer (BioTek, USA). The optical densities of each virus-containing well was read at 450nm using the modulus microplate multimode reader (Turner Biosystems, New York, USA).

For some of the mutant viruses, levels of p24 could not be detected at the abovementioned dilution, therefore the dilutions were adjusted accordingly and measurement of p24 repeated. The concentration of p24 levels in the mutant viruses were calculated using the standard curve. The curve was a plot of the concentration of the HIV-1 p24 Antigen standard (x axis), which was included in every assay, against the optical densities for each standard.

2.7 Replication capacity assay

The replication capacity assay was performed as previously described (151). The assay was performed twice independently using two different donor PBMCs. The PBMCs were previously obtained from South African National Blood Services and cryopreserved at HPP. A negative (ΔNef) and positive control (SF2 Nef) was included in every assay.

2.7.1 Thawing of PBMCs

PBMCs were thawed one day before infection by removing a vial of cells from storage in liquid nitrogen and immediately suspending the vial in a 37 °C waterbath. Once thawed, the cells were made up to 20 ml with R10 (RPMI 1640 [Sigma] with L-glutamine [Invitrogen], 1 % MEM non-essential AA [Gibco], 1 % of 100 mM sodium pyruvate [Gibco], 10 % FBS [Gibco]) and centrifuged at 1500 rpm for 5 minutes. The supernatant was removed and the cells re-suspended in 10 ml of R10 and again centrifuged at 1500 rpm for 5 minutes. The cells were once again re-suspended in 10 ml of R10 and the cells were cultured at 37 °C and 5% CO_2 until infection the next day.

2.7.2 Infection of PBMCs

A cell count was performed using a hemocytometer by mixing 10 µl of the PBMC culture with 10 µl of trypan blue (0.4 %) and loading 10 µl of the mixture into the chamber of a hemocytometer. The cells were then viewed and counted using the microscope. Only the live cells were counted. Live cells were differentiated by the uptake of the blue dye by dead cells.

The calculated volume of culture, i.e. the volume which contained one million PBMCs, was dispensed into 15 ml tubes and the cells pelleted by centrifugation at 1500 rpm for 10 minutes. The supernatant was removed and the cells re-suspended by gently pipetting in the appropriate volume of R10 such that the added volume of media and virus was 800 µl. The correct volume of virus, which contained 7.5 ng p24 antigens, was added to the cell suspension. This was then mixed four times by pipette and spinoculated (centrifugation at 1000 rpm and 4 ℃ for 30 minutes) to enhance infection (127, 130). When complete, this was very gently mixed by pipetting and was incubated at 37 °C and 5% CO_2 for 7 hours. Upon completion of the incubation, 10ml of warm R10 was added to each sample tube and centrifuged at 22 ℃ and 1500 rpm for 5 minutes. The supernatant was discarded and the pellet re-suspended in 400 µl R10. This was equally divided into 4 wells of a 96 well plate. The same tube was then washed with another 400 µl of R10 and again divided equally into the same wells. At the end, for each sample, 4 wells each contained 200 µl of medium which in turn contained 250000 cells with infected virus. The plate was incubated at 37 ℃ and 5 % CO_2 for 12 days.

2.7.3 Activation of infected PBMCs

Cell proliferation was stimulated on day 3 of incubation with phytohaemagglutinin (PHA; [Sigma]). Firstly, 100 ul of the viral supernatant was removed from the culture plate and discarded. Next, PHA was diluted with R10 to 10 µg/ml and 100 µl of PHA-containing media was added into each of the sample wells such that the final concentration of PHA within each well was 5µg/ml. On day 6 and every 3 days following, 100 µl of the viral supernatant was removed from the culture plate and stored in 96 well plates at -80 °C. Following the removal of viral supernatant, the cells were stimulated with 100 µl of R10 containing interleukin-2 (IL-2,

Roche, USA) at a concentration of 20 U/ml IL-2, in the same way as described for PHA above (resulting in a final concentration of 10 U/ml IL-2 in each well).

Viral replication ability was determined by measuring the p24 levels of the day 12 viral supernatants by ELISA as described in Section 2.6. Day 12 was the optimal time to measure replication as all the viruses had detectable replication but none of the viruses had passed peak replication.

2.8 Cloning of the mutant *nef* sequences into pselect plasmid

Prior to measuring the Nef-mediated CD4 and HLA-I down-modulation capacities of the mutated Nef proteins in a T cell line, the mutant *nef* sequences were cloned, as previously described (106), into a zeocin-resistant GFP-expressing plasmid (pselect) as this allowed detection by flow cytometry of cells transfected with Nef clones. The pselect plasmid (Invivogen) was modified by insertion of a linker region containing AscI and SacII restriction enzyme sites and kindly donated by Dr. Mark Brockman. The cloning process is described below and illustrated in Figure 2.5.

2.8.1 PCR amplification of mutant *nef* sequences

The mutated *nef* sequences (generated by mutagenesis (Section 2.4.) were amplified using the Roche Expand High Fidelity PCR system (Roche) as described in Section 2.3.1.

Figure 2.5. CD4 and HLA down-modulation assay

The mutant *nef* gene was amplified with forward and reverse primers containing AscI and SacII restriction sites, respectively. The amplified mutant *nef* and a plasmid modified to contain AscI and SacII restriction sites were digested with AscI and SacII restriction enzymes. These products were then ligated using T4 DNA ligase. The plasmid was then transformed into E. Cloni cells and plated on LB-zeocin plates to select for cells transformed with zeocin-resistant plasmids. Plasmid DNA was purified from a single colony using a mini-prep procedure. A restriction digest which was gel electrophoresed as well as sequencing were performed to confirm the presence of the *nef* insert.

The Nef clones were transfected into GXR cells modified to express high levels of HLA-A*02. Following a 20-hour incubation, the cells were stained with fluorochrome-conjugated antibodies which bind to CD4 (APC-labelled anti-CD4 antibody) and HLA-I (PE-labelled HLA-A*02 antibody) molecules to allow for measurement of these molecules by flow cytometry.

Mutant nef gene PCR amplified with primers containing AscI and SacII sites

Amplified mutant nef gene and pselect plasmid digested with Asc-I and Sac-II

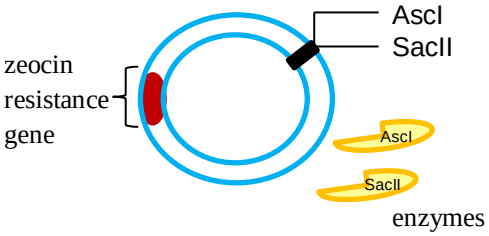

Digested nef gene ligated into linearised pselect with T4 DNA ligase

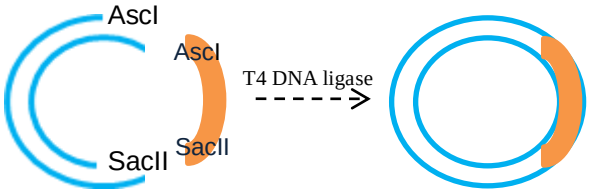

Ligated product transformed

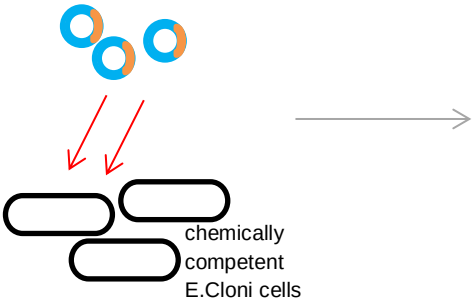

chemically competent E.Cloni cells

Transformed cells – plated on LB zeocin plates

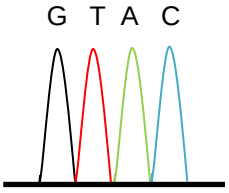

Sequenced to confirm presence of the correct mutant *nef* sequence

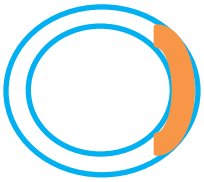

Plasmid DNA was puirified by a miniprep procedure

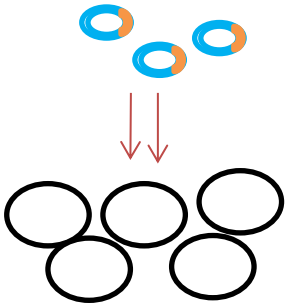

CEM-GXR cells which express high levels of HLA-A*02 – transfected with plasmid DNA

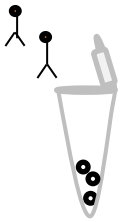

cells stained with fluorochrome-conjugated antibodies which bind to CD4 and HLA- these molecules were measured by flow cytometry

The forward (5' AGAGCACC**GGCGCGCC**TCCACATACCTASAAGAATMAGACARG 3',AscI site in bold) and reverse (5' GCCT**CCGCGG**ATCGATCAGGCCACRCCTCCCTGGA AASKCCC 3', SacII site in bold) primers used contained AscI and SacII restriction sites, respectively. The mutated *nef* amplicons were PCR purified as described in Section 2.3.2.3.

2.8.2 Digestion of mutated *nef* amplicons and pselect plasmid

Purified mutated *nef* amplicons (500 ng) and pselect plasmid (5 µg) were both digested with restriction enzymes Asc-I (5 U) and Sac-II (5 U) (New England Biolabs) in the presence of Buffer 4 (1 ×) and water added to a final volume of 20 µl. The reaction was incubated at 37 °C for 1 hour and the enzyme inactivated at 65 °C for 20 minutes. The digested pselect plasmid was electrophoresed in the presence of TAE buffer, excised from the gel and purified as described in Section 2.3.2

2.8.3 Ligation of digested *nef* amplicons and pselect plasmid

The ligation of digested *nef* amplicons (90 ng) and pselect plasmid (100 ng) was performed as described in Section 2.3.3. Thereafter, ligated products were transformed into E.cloni cells and amplified by colony PCR to determine the presence of Nef in the plasmid clone (as described in Sections 2.3.4.1). The nef-containing colonies were then sequenced (Section 2.3.4.2) to verify the presence of the correct sequence. The colonies containing the clone with the correct sequence were cultured in 3 ml LB-zeocin broth (25 µg zeocin per ml LB broth) at 37 °C and 250 rpm for 2 hours. The culture was then split in half, supplemented with 1 ml LB-zeocin broth and

similarly incubated overnight. The plasmid DNA was purified using the GeneJET plasmid Miniprep kit (Thermo Scientific, USA) according to manufacturer's indications.

2.9 CD4 and HLA-I down-modulation assays

Nef-mediated CD4 and HLA-I down-modulation was performed as previously described (106) in a GXR cell line which expresses high levels of CD4 and was modified to express high levels of HLA-A*02 (donated by Dr. Mark Brockman). Previous measurements of Nef-mediated HLA-A*02 and HLA-B*07 down-modulation for 21 Nef clones were highly correlated ($r=0.82$ and $p<0.0001$) (106). It is therefore likely that Nef's ability to down-modulate HLA-A*02 is a general representative of Nef's ability to down-modulate both HLA-A and HLA-B molecules.

The cells were counted as described in Section 2.5.2 and 600000 cells per sample were pelleted by centrifugation at 1500 rpm for 10 minutes. The cells were re-suspended in MegaCell medium (RPMI 1640medium without L-glutamine [Sigma]) and 250 µl media which contained 600000 cells was transferred into electroporation cuvettes. To this, 8 µg of the mini-prepped Nef clone (Section 2.8.3.), diluted in 150 µl MegaCell media, was added and mixed by gentle pipetting. Thereafter, electroporation was carried out at 250 V and 950 µF. The transfected cells were rested for 10 minutes after electroporation and supplemented with 500 µl R10 medium. The cuvette contents were then evenly distributed between two cluster tubes which contained 250 µl of R10 medium. The samples were incubated in a cluster tube box, sealed ajar, at 37 °C and 5 % CO_2 for 20 hours.

The samples were then centrifuged at 1500 rpm for 10 minutes and the supernatant discarded. Each sample was stained with 2 µl APC-labelled anti-CD4 antibody (BD Biosciences, San Jose, USA)) and 3 µl PE-labelled HLA-A*02 (BD Biosciences, San Jose, USA) antibody, stabilised in phosphate buffered saline solution (PBS [Gibco]). The antibody stained samples were incubated at 4 °C for 10 minutes before being washed with the addition of 750 µl PBS and centrifugation at 1500 rpm for 10 minutes. The supernatant was again removed by pipette and the cells fixed by the addition of 300 µl of 2 % PFA. The mixture was vortexed for 15 seconds and incubated at 4 °C for 10 minutes. This was followed by incubation at room temperature for 45 minutes and measurement of Nef mediated CD4 and HLA-I down-modulation of each mutant viral strain was performed by flow cytometry (Figure 2.5)

To determine the relative CD4/HLA down-modulation capacities of each mutant Nef, the mean fluorescence intensity (MFI) of CD4 and HLA expression were normalised to the MFI for the negative (ΔNef clone) and positive (SF2 Nef plasmid clone) controls, included in every assay, such that normalised MFI values of 0 % and 100 % represented no down-modulation activity and down-modulation activity equivalent to the positive control, respectively. This was done using the following equation: (negative control – mutant Nef) ÷ (negative control – positive control). Assays were performed in two independent experiments with duplicate measurements in each experiment. The duplicate results were averaged.

2.10 Data analysis

The relationship between the predicted fitness costs of the mutant viruses (expressed as E values) and the measured replication capacities of the mutant viruses were evaluated using Pearson's correlation or Spearman's rank correlation for normally distributed and skewed data, respectively. In addition, the relationship between the predicted fitness costs and the measured Nef-mediated CD4 and HLA-I down-modulation capacities were similarly evaluated. A significance level of $p<0.05$ was used for all statistical analyses.

CHAPTER 3

RESULTS

3.1 Introduction

Nef is an important factor in HIV-1 pathogenesis as well as host immune evasion (19, 39, 53, 78). Although Nef is known to be an important HIV-1 virulence factor; and was included in the unsuccessful STEP trial, there is little evidence for or against its inclusion in vaccine strategies (21). Computational models, namely Ising and Potts, have been developed with the ability to predict the viral fitness landscape of different HIV-1 proteins and in so doing could reveal vulnerabilities within the Nef protein and indicate suitability of its inclusion in an HIV vaccine (49). However, these models need to be validated by *in vitro* experiments and experiments using animal models (49).

This study aimed to evaluate and compare the accuracy of the Ising and Potts models in predicting the fitness consequences of mutations in HIV-1 Nef. In order to do so, we performed *in vitro* measurements of the Nef-driven replication capacities as well as CD4 and HLA down-modulation capacities of 32 mutants (data in Table 3.1), which were selected based on their energies (E) predicted by the models.

Table 3.1. *In vitro* measurements of the replication capacities, CD4 down-modulation capacities and HLA down-modulation capacities of the 32 selected mutants

Category	Mutant	Ising E	Potts E		Replication capacity (%)	CD4 down-modulation (%)	HLA down-modulation (%)
				Previously shown to be required for down modulation of:			
Known functional motifs	17K19K	10.15	10.60	HLA and to a lesser extent CD4 (141)	26.10	101.3	94.40
	57G	6.60	6.73	CD4 (60, 67, 104)	0.90	13.80	100.3
	57R	6.60	5.16	CD4 (60, 67, 104)	0.80	51.10	101.7
	57R58P	10.70	9.67	CD4 (60, 67, 104)	0.10	22.20	102.6
	72L75L	12.85	13.92	HLA (52, 104)	7.50	65.30	54.0
	123G	5.95	7.48	HLA and CD4 (52, 60)	6.40	28.70	32.0
HLA associated/ CTL escape mutants and mutant pairs	28E	-0.20	1.43		85.10	99.10	97.70
	33A	1.11	1.89		129.3	100.2	100.5
	43L	1.45	4.16		69.40	97.20	103.8
	71K	1.60	1.48		85.40	100.2	97.20
	76V	3.72	4.95		84.30	100.6	93.10
	80D	3.74	6.07		18.60	90.0	96.60
	80N	3.74	4.52		83.20	96.50	1.006
	88G	3	8.94		87.0	99.70	94.10
	102H	-0.60	0.98		46.60	97.0	88.70
	102W	-0.60	4.28		75.40	100.8	80.40
	133T	-0.97	0.8		59.90	99.40	90.70
	135F	0.92	2.23		114.3	100.3	97.40
	143Y	3.57	2.88		94.10	97.80	99.0
	188H	1.55	2.72		68.90	0.989	97.0
	192R	0.99	2.47		No result[b]	100.8	98.5
	28E102H	0.43	2.60		139.4	No result[b]	No result[b]
	28E102W	0.43	6.10		82.90	100.2	98.60
	33A43L	1.47	2.87		88.10	98.0	98.20
	43L88G	5.40	13.29		91.60	94.70	96.40
	71K76V	6.53	6.57		106.5	102.6	93.70
	76V80N	8.16	9.62		53.10	96.60	86.80
	133T135F	-1.22	0.58		146.3	100.3	96.70
	135F143Y	7.56	6.28		103.4	97.30	96.10
	188H192R	1.74	2.61		56.0	99.50	96.80

Variable amino acids at same codon	21E	-0.34	5.31	146.4	101.7	97.70
	21K	-0.34	0.58	51.50	101.4	96.10
	57G[a]	6.60	6.73	0.90	13.80	100.3
	57R[a]	6.60	5.16	0.80	51.10	101.7
	80D[a]	3.74	6.07	18.60	90.0	96.60
	80N[a]	3.74	4.52	83.20	96.50	100.6
	102H[a]	-0.60	0.98	46.60	97.0	88.70
	102W[a]	-0.60	4.28	75.40	100.8	80.40
	28E102H[a]	0.43	2.60	139.4	No result[b]	No result[b]
	28E102W[a]	0.43	6.10	82.90	100.2	98.60

[a]Mutants repeatedly listed in the Table i.e. mutants which fall into more than one category

[b]These results were unobtainable due to unsuccessful cloning of mutants 192R into the NL4-3 plasmid and 28E102H into the pselect plasmid (Section 3.2 and 3.3)

3.2 Measurement of the replication capacities of mutant viruses

Mutations were introduced by site-directed mutagenesis into the consensus B *nef* gene (which was cloned into a HIV-1 NL4-3 plasmid), and the presence of mutations were confirmed by sequencing. The cloning of mutant 192R into the NL4-3 plasmid was unsuccessful, thus the replication capacity of this mutant was not determined. Although several attempts were made to clone 192R into the NL4-3 plasmid, spontaneous mutations were observed each time, which is a challenge associated with the cloning process (96). In addition, it is possible that *in vivo*, this mutant is only found in combination with other specific mutations in or outside *nef* or that it is inherently unstable in the bacterial cloning system. Further studies to verify these hypotheses may be required. Due to the uncertain time frame of generating this clone and experimental constraints (functional/replication assays should ideally be performed in a batch alongside the wild-type Nef), this clone was excluded from further replication analysis. For the rest of the mutants, virus stocks were generated by electroporation of a GFP-reporter T cell line with mutant plasmids. The replication capacities of the mutant viruses were then determined by infection of PBMCs and by the measurement of p24 levels by ELISA. The replication capacities of the mutant viruses were normalised to that of the wild-type virus and are shown in Table 3.1.

3.2.1 Reproducibility of results

The experiments were performed in duplicate using PBMCs from two different donors and the mean of the results are presented in Table 3.1. The replicates of this experiment were in good concordance (Pearson $r = 0.7780$, $p = <0.0001$) (Figure 3.1).

Figure 3.1. Graph depicting the relationship between the replicates of the replication capacity assay

A Pearson's correlation was performed and yielded r = 0.7780 and p = <0.0001 which indicated a strong significant correlation between replicate measurements of the replication assay performed in peripheral blood mononuclear cells (PBMCs) from two different donors.

RC - *In vitro* replication capacities of the mutant viruses normalised to that of the wild-type virus (100 %)

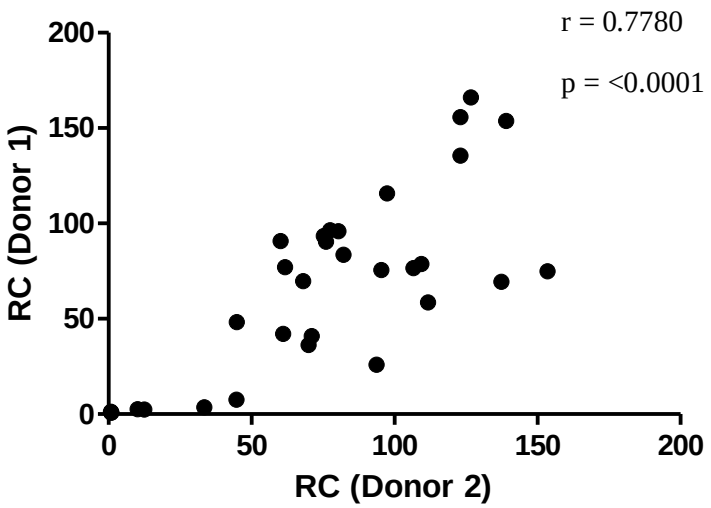
r = 0.7780
p = <0.0001
RC (Donor 1)
RC (Donor 2)
0
50
100
150
200

3.2.2 Relationships between E values predicted by the Ising and Potts models and replication capacities of mutant viruses

Correlations were performed to evaluate and compare the accuracy of the Ising and Potts models in predicting the fitness consequences of mutations. To evaluate the accuracy of the Ising model, a correlation was performed between the E values predicted by the Ising model and replication capacities (Figure 3.2A). The Potts model was similarly evaluated (Figure 3.2B). The data was normally distributed in both data sets; therefore Pearson's correlations were done.

There was a significant negative correlation ($r = -0.5793$, $p = 0.0006$) between the E values predicted by the Ising model and the mutant replication capacities (Figure 3.2A). There was also a significant negative correlation ($r = -0.4118$, $p = 0.0213$) between the E values predicted by the Potts model and the replication capacities (Figure 3.2B). It was shown that the correlation was stronger between the Ising predicted E values and replication capacities than that between the Potts predicted E values and replication capacities ($r = -0.5793$ vs. $r = -0.4118$, respectively).

Figure 3.2. Relationship between *in vitro* replication capacities of mutant viruses and predicted fitness costs (expressed as E values)

(A) Graph showing a negative correlation ($r = -0.5793$, $p = 0.0006$) between replication capacities of mutant viruses and fitness costs predicted by the Ising model.

(B) Graph showing a negative correlation ($r = -0.4118$, $p = 0.0213$) between replication capacities of mutant viruses and fitness costs predicted by the Potts model.

RC – *In vitro* replication capacities of the mutant viruses normalised to that of the wild-type virus (100 %)

A

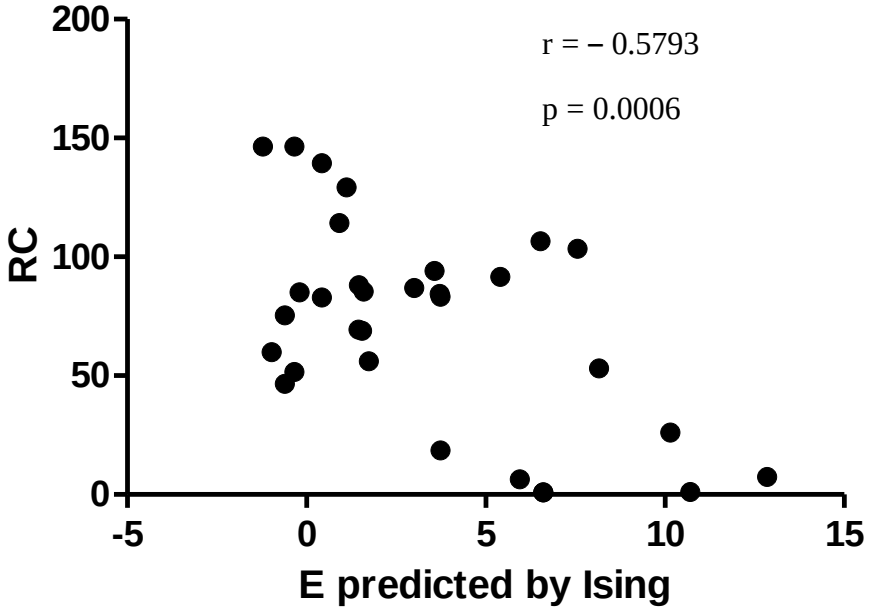
r = – 0.5793
p = 0.0006
RC
200
150
100
50
0
-5
0
5
10
15
E predicted by Ising

B

12

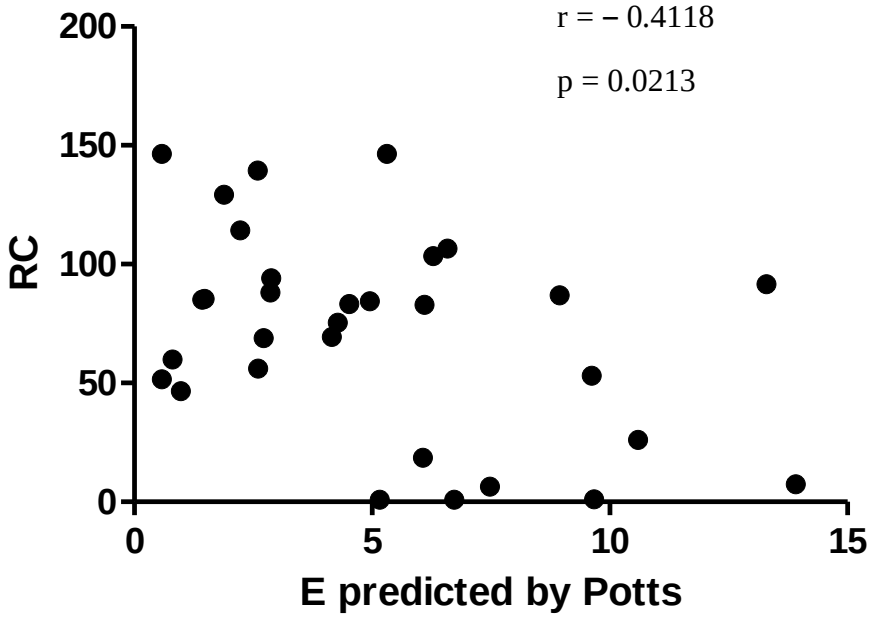
r = – 0.4118
p = 0.0213
RC
200
150
100
50
0
0
5
10
15
E predicted by Potts

3.3 Measurement of the ability of Nef mutants to down-modulate CD4 and HLA

Nef may enhance HIV-1 pathogenesis through activities such as CD4 down-modulation which improves HIV-1 infectivity and replication. In addition, Nef may also enhance HIV-1 pathogenesis through CD4-independent mechanisms, such as HLA-I down-modulation which increases immune evasion (53). Therefore we also tested the effect of Nef mutations on these two well-studied functions of Nef.

The mutant *nef* sequences were cloned into a GFP-expressing pselect plasmid. The presence of all mutations was confirmed by sequencing except for mutant 28E102H. As was the case for 192R, several attempts at cloning were made but spontaneous mutations were being introduced (96), and this clone was therefore excluded from down-stream analysis. GXR cells expressing high levels of HLA-A*02 were transfected with the 31 clones (all mutant Nef clones except the 28E102H mutant) and cell surface expression of CD4 and HLA-A*02 in transfected cells was measured by flow cytometry. The down-modulation capacities of the mutant Nef clones were indicated by median fluorescence intensity relative to that of the positive and negative controls. This value was then normalised to that of the wild-type Nef and these measurements are presented in Table 3.1. Representative flow cytometry plots are illustrated in Figure 3.3.

Figure 3.3. Representation of the flow cytometric measurements of Nef-mediated CD4 and HLA down-modulation

Graphs show the HLA-A*02 and CD4 cell surface expression on the Y axis and green fluorescent protein (GFP) expression is indicated on the X axis of graphs. GFP-positive cells represent cells successfully transfected with the Nef clones. HLA-A*02 and CD4 cell surface expression was measured in GFP-positive cells.

(A) and (B) Graphs representing HLA-A*02 down-modulation (A) and CD4 down-modulation (B), respectively, of the negative control (ΔNef). The negative control represents no down-modulation ability.

(C) and (D) Graphs representing HLA-A*02 down-modulation (C) and CD4 down-modulation (D), respectively, of the positive control (SF2 Nef). The positive control represents 100% down-modulation ability.

(E) and (F) Graphs depicting intermediate HLA down-modulation capacity (E) and CD4 down-modulation capacity (F) by mutant 72L75L. It is shown that this mutant down-modulated HLA 54% and CD4 65.3% relative to the positive and negative controls.

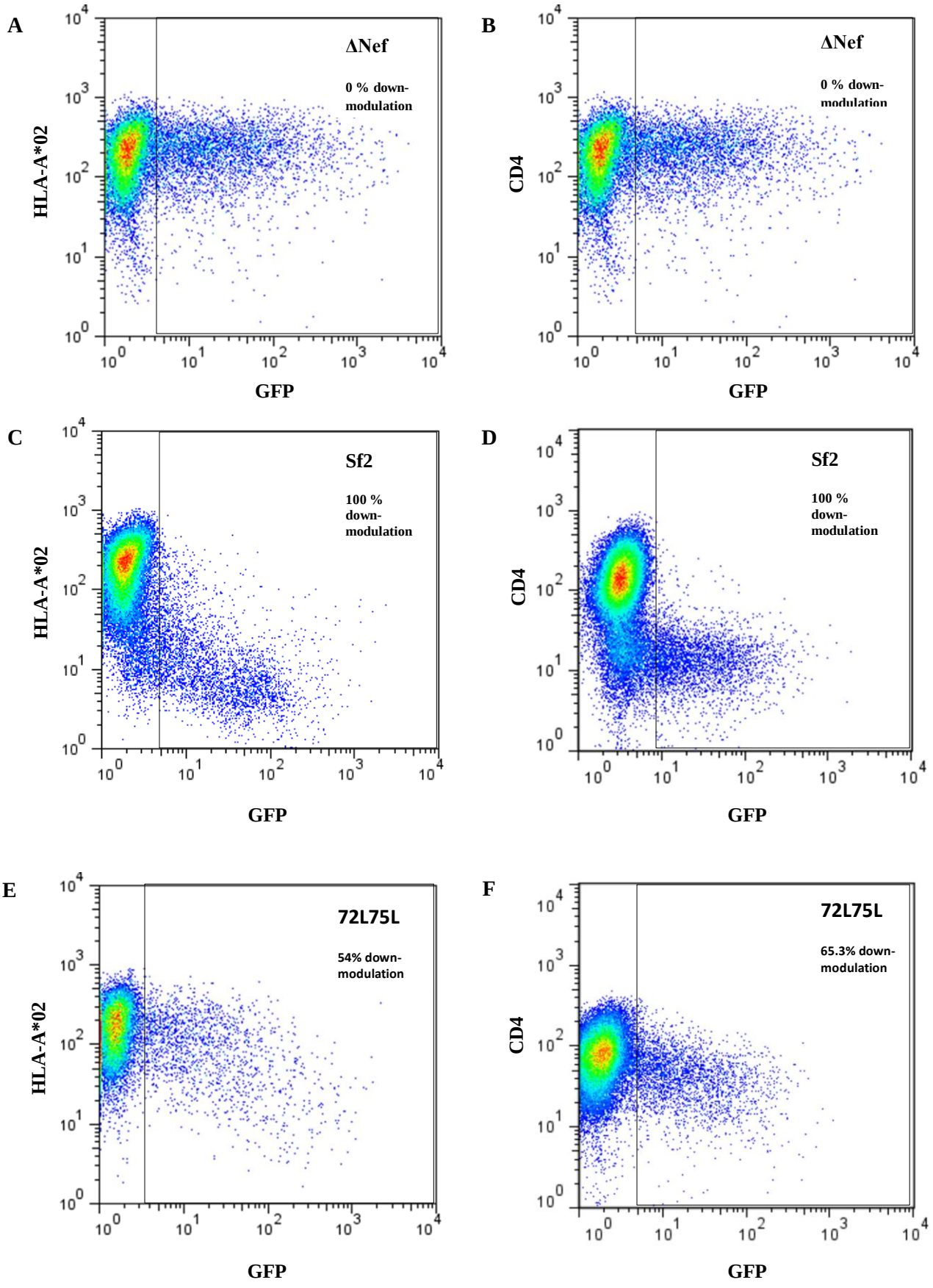
A
ΔNef
0 % down-modulation
HLA-A*02
GFP
B
ΔNef
0 % down-modulation
CD4
GFP
C
Sf2
100 % down-modulation
HLA-A*02
GFP
D
Sf2
100 % down-modulation
CD4
GFP
E
72L75L
54% down-modulation
HLA-A*02
GFP
F
72L75L
65.3% down-modulation
CD4
GFP

3.3.1 Reproducibility of results

All the experiments were performed in duplicate and the mean of the results are presented in Table 3.1. The replicates of these experiments were in agreement (Spearman: $r = 0.7780$, $p = <0.0001$ and $r = 0.4609$, $p = 0.0091$) (Figure 3.4).

Figure 3.4. Graphs depicting the relationships between the replicates of CD4 and HLA down-modulation measurements

Spearman's correlations were performed between replicates for both CD4 down-modulation (Figure 3.4A) and HLA-A*02 down-modulation (Figure 3.4B). These yielded $r = 0.7809$, $p = <0.0001$ and $r = 0.4609$, $p = 0.0091$, respectively, which indicated a significant correlation between replicate measurements of the assays performed.

A

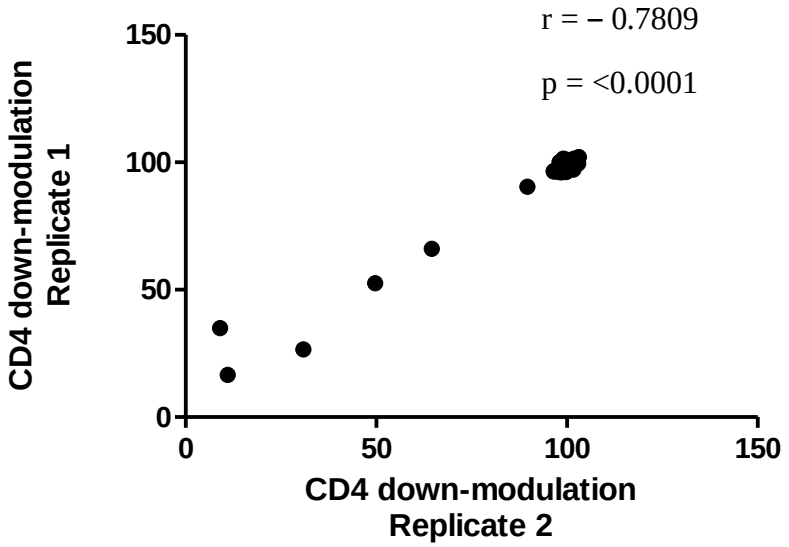
r = – 0.7809
p = <0.0001
CD4 down-modulation Replicate 1
CD4 down-modulation Replicate 2
0
50
100
150

B

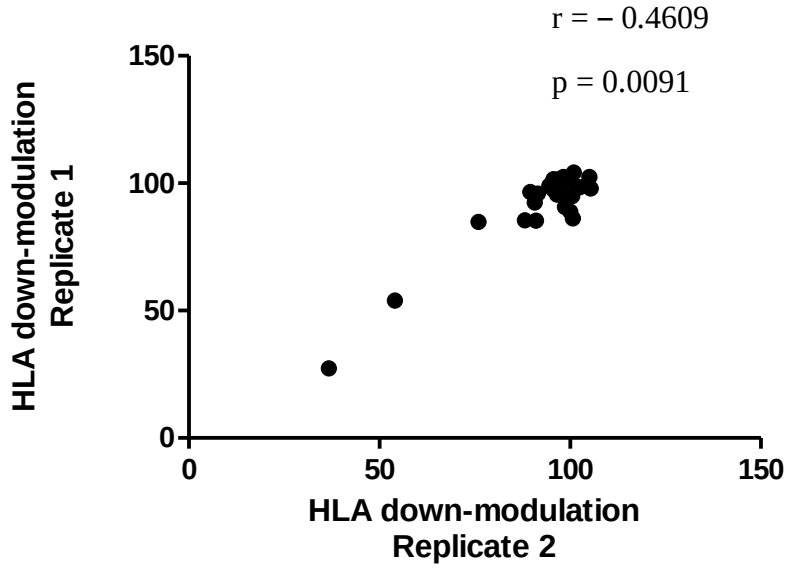
r = – 0.4609
p = 0.0091
HLA down-modulation Replicate 1
HLA down-modulation Replicate 2
0
50
100
150

3.3.2 Relationships between the E values predicted by the Ising and Potts models and the CD4/HLA down-modulation capacities of mutant Nef clones

Correlations were performed between the mutant E predicted by the Ising model and the CD4 and HLA-A*02 down-modulation capacities (Figure 3.5A and -B, respectively). Similar correlations were performed for predictions made by the Potts model (Figure 3.5C and -D). The data was skewed in all data sets; therefore a Spearman's rank correlation was done in each instance.

There was a significant negative correlation between the CD4 down-modulation capacities and the E values predicted by the Ising model ($r = -0.5266$, $p = 0.0023$, Figure 3.5A) as well as the E values predicted by the Potts model ($r = -0.3781$, $p = 0.0360$, Figure 3.5C). However, the correlation was stronger with the Ising model than with the Potts model ($r = -0.5266$ with Ising and $r = -0.3781$ with Potts). For both models, substantial reductions in CD4 down-modulation are only observed at E values >5. The mutants with E>5 which display reduced CD4 down-modulation are: 57G, 57R, 57R58P, 72L75L and 123G. Interestingly, 57G, 57R, 57R58P and 123G are in motifs known to affect CD4 down-modulation (Table 3.1).

There was no correlation between the HLA down-modulation capacities and the E values predicted by the Ising model ($r = -0.03469$, $p = 0.8530$) as well as the E values predicted by the Potts model ($r = -0.1676$, $p = 0.3676$) (Figure 3.5B and -D). It should be noted, however, that only two mutants displayed reduced HLA-A*02 down-modulation, namely 72L75L and 123G.

Figure 3.5. Relationships between *in vitro* Nef-mediated CD4 and HLA down-modulation capacities of mutant Nef clones and predicted fitness costs (expressed as E values)

(A) Graph showing a significant negative correlation ($r = -0.5266$, $p = 0.0023$) between CD4 down-modulation capacities of mutant Nef clones and fitness costs predicted by the Ising model.

(B) Graph showing no correlation ($r = -0.03469$, $p = 0.8530$) between HLA down-modulation capacities of mutant Nef clones and fitness costs predicted by the Ising model.

(C) Graph showing a significant negative correlation ($r = -0.3781$, $p = 0.0360$) between CD4 down-modulation capacities of mutant Nef clones and fitness costs predicted by the Potts model.

(D) Graph showing no correlation ($r = -0.1676$, $p = 0.3676$) between HLA down-modulation capacities of mutant Nef clones and fitness costs predicted by the Potts model.

Nef-mediated CD4 and HLA down-modulation capacities of the mutant Nef clones were normalised to that of the wild-type Nef (100 %)

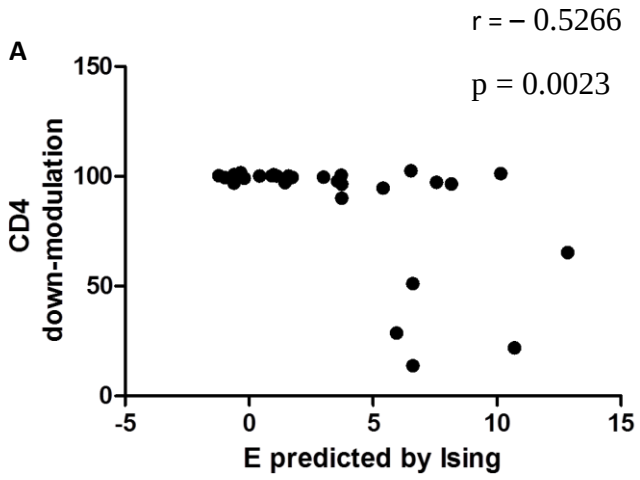
A
r = – 0.5266
p = 0.0023
CD4
down-modulation
150
100
50
0
-5
0
5
10
15
E predicted by Ising

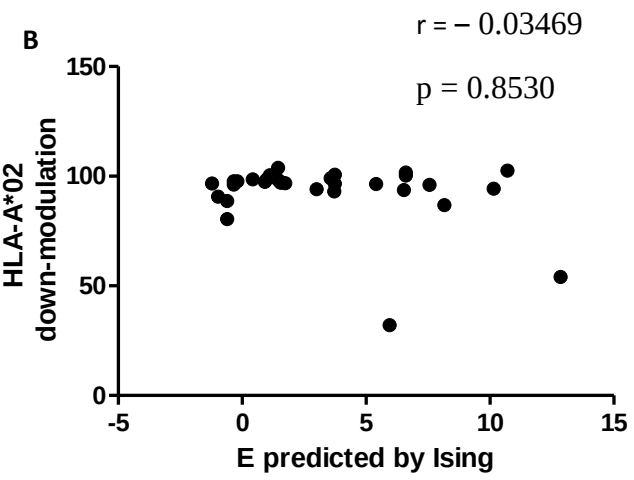
B
r = – 0.03469
p = 0.8530
HLA-A*02
down-modulation
150
100
50
0
-5
0
5
10
15
E predicted by Ising

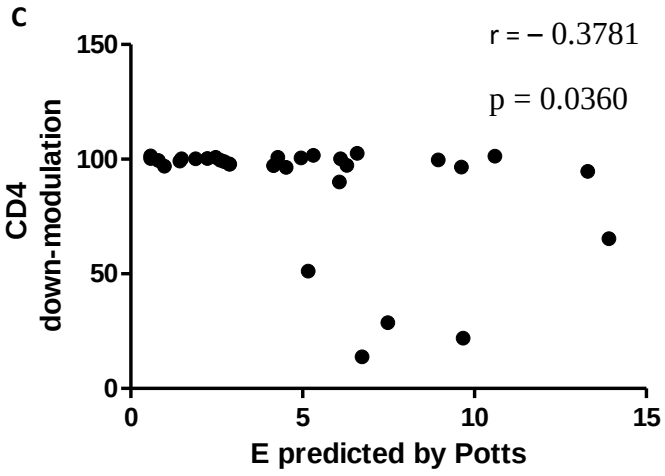
C
r = – 0.3781
p = 0.0360
CD4
down-modulation
150
100
50
0
0
5
10
15
E predicted by Potts

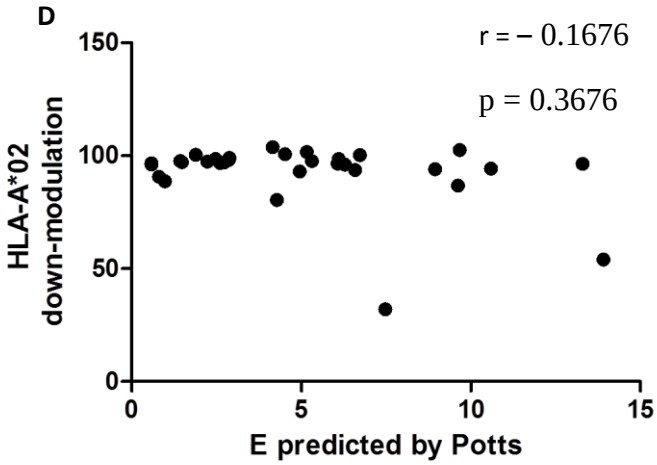
D
r = – 0.1676
p = 0.3676
HLA-A*02
down-modulation
150
100
50
0
0
5
10
15
E predicted by Potts

3.4 Relationships between replication capacities and CD4/HLA down-modulation capacities

The relationships between the replication capacities and the CD4/HLA down-modulation capacities were explored by performing correlations. The data sets, in both cases, were not normally distributed; therefore Spearman's rank correlations were conducted. These correlations excluded mutants 192R and 28E102H for reasons mentioned in Section 3.2 and Section 3.3, respectively.

As shown in Figure 3.6, there was a significant positive correlation ($r = 0.5778$ and $p = 0.0008$) between the replication capacities and the Nef-mediated CD4 down-modulation capacities (A). However, there was no correlation between the replication capacities and Nef-mediated HLA down-modulation capacities ($r = 0.2076$ and $p = 0.2711$) (B).

Figure 3.6. Relationships between *in vitro* replication capacities and Nef-mediated CD4/HLA down-modulation capacities

(A) Graph showing a significant positive correlation (r = 0.5778 and p = 0.0008) between replication capacities and CD4 down-modulation capacities.

(B) Graph showing no correlation (r = 0.2076 and p = 0.2711) between replication capacities and HLA down-modulation capacities.

In vitro replication capacities (RC) as well as Nef-mediated CD4 and HLA down-modulation capacities of the Nef mutants were normalised to that of the wild-type Nef (100 %)

A

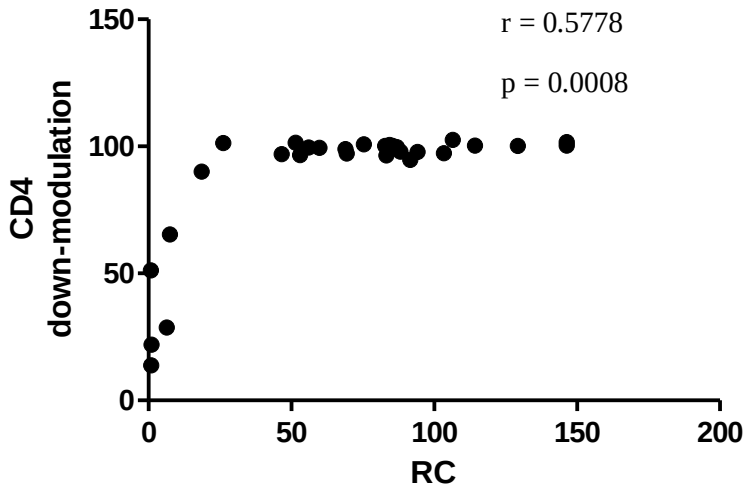
r = 0.5778
p = 0.0008
CD4
down-modulation
150
100
50
0
0
50
100
150
200
RC

B

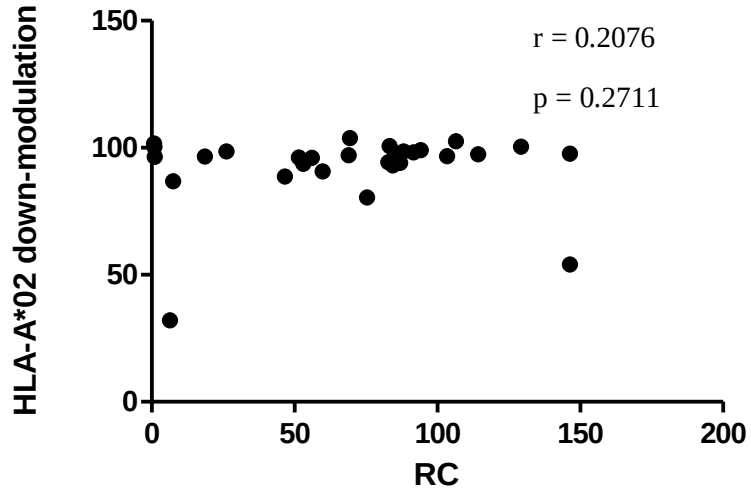
r = 0.2076
p = 0.2711
HLA-A*02 down-modulation
150
100
50
0
0
50
100
150
200
RC

3.5 Overview of data by category

The data was additionally analysed according to the categories of mutants listed in Table 3.1.

3.5.1 Known functional motifs

Mutants under this category were selected for their known ability to affect one or more functions of Nef (Table 3.1). Under the category of known functional motifs, all mutants had a substantially reduced replication capacity relative to the wild-type, ranging between 0.1 and 26.1 % (Table 3.1 and Figure 3.7). Also, all these mutants, with the exception of 17K19K, displayed an impaired ability to down-modulate CD4: the ability of the other mutants (57G, 57R, 57R58P, 72L75L and 123G) to down-modulate CD4 was 13.8 – 65.3 % of wild-type levels. These mutants, with the exception of 72L75L, were previously noted in the literature to be important for CD4 down-modulation activity (Table 2.1 and 3.1). Also consistent with the literature, mutants 57G, 57R and 57R58P retained the ability to down-modulate HLA (100 - 102% of wild-type levels) while CD4 down-modulation activity was lessened, and 123G was impaired for both CD4 and HLA down-modulation (28.7 % and 32 %, respectively). Mutations in motifs previously shown to be required for HLA down-modulation (Table 2.1 and 3.1) also showed reduced HLA down-modulation relative to the wild-type virus, although for mutant 17K19K, HLA down-modulation was only slightly reduced. Mutants 17K19K, 72L75L and 123G displayed a 94.4 %, 54 % and 32 % ability to down-modulate HLA, respectively.

Figure 3.7. Replication capacities as well as Nef-mediated CD4 and HLA down-modulation abilities of mutants which fall into the category of known functional motifs

The bars displayed in the graph are representative of the mean of replicates for the mutants replication capacities (blue) as well as CD4 down-modulation (grey) and HLA-A*02 down-modulation capacities (red). Previously, it was shown that following mutants were required for the down-modulation of: HLA and to a lesser extent CD4 (17K19K); CD4 (57G, 57R and 57R58P); HLA (72L75L); HLA and CD4 (123G).

In vitro replication capacities (RC) as well as Nef-mediated CD4 and HLA down-modulation capacities of the Nef mutants were normalised to that of the wild-type Nef (100 %)

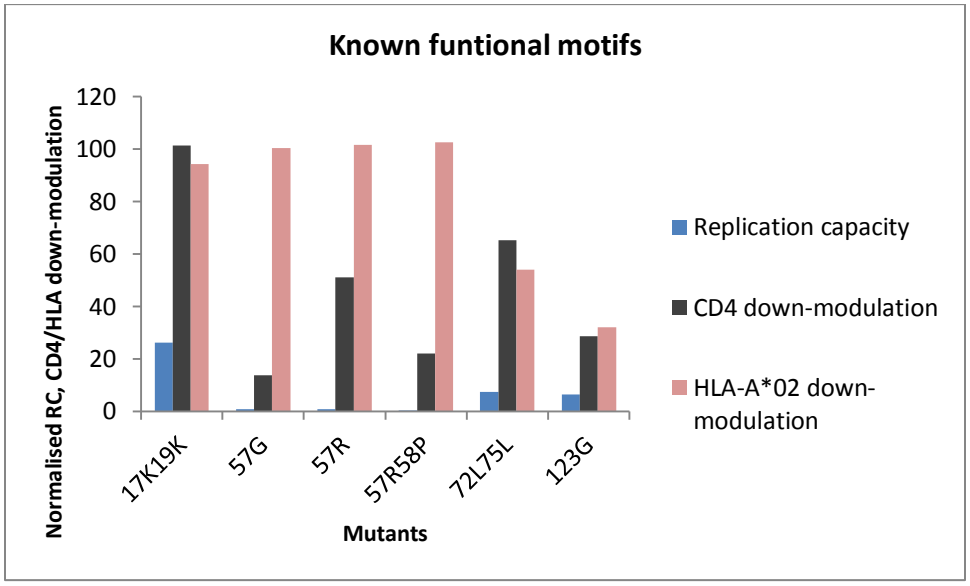
Known funtional motifs
Normalised RC, CD4/HLA down-modulation
120
100
80
60
40
20
0
17K19K
57G
57R
57R58P
72L75L
123G
Mutants
Replication capacity
CD4 down-modulation
HLA-A*02 down-modulation

3.5.2 HLA associated/escape mutants and mutation pairs

HLA-associated mutations (likely cytotoxic T cell escape mutants) or known escape mutants, as well as pairs of these mutations, were selected that covered a range of E values. Only one of the mutants in this category displayed a marked reduction in replication capacity, namely 80D (18.6 % of wild-type levels), while the rest ranged from 46.6 – 146.3 % of wild-type levels (median of 85.1%) (Table 3.1 and Figure 3.8A). Overall, CD4 and HLA down-modulation capacities of mutants in this category were largely similar to wild-type (Table 3.1 and Figure 3.8B). The CD4 down-modulation capacities ranged from 90 to 102.6 % of wild-type levels (median of 99.4 %) and HLA down-modulation capacities from 80.4 – 103.8 % of wild-type levels (median of 96.8 %).

Figure 3.8. Replication capacities as well as CD4 and HLA down-modulation capacities of mutants which fall into the category of HLA associated/escape mutants (A) and mutant pairs (B)

The bars displayed in the graph are representative of the mean of replicates for the mutants replication capacities (blue) as well as CD4 down-modulation (grey) and HLA-A*02 down-modulation capacities (red).

In vitro replication capacities (RC) as well as Nef-mediated CD4 and HLA down-modulation capacities of the Nef mutants were normalised to that of the wild-type Nef (100 %)

The asterisk indicates missing data.

A

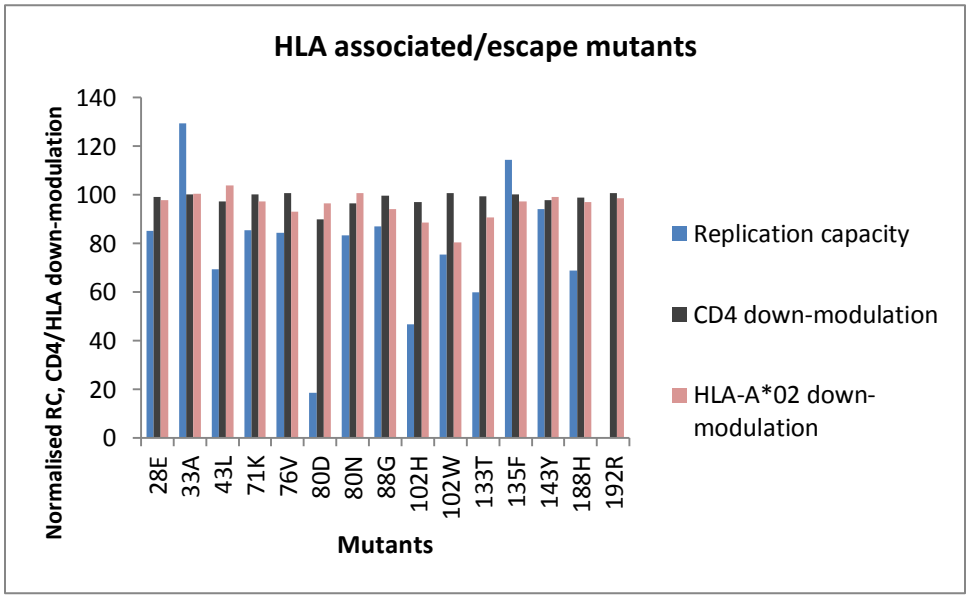
HLA associated/escape mutants
Normalised RC, CD4/HLA down-modulation
140
120
100
80
60
40
20
0
28E
33A
43L
71K
76V
80D
80N
88G
102H
102W
133T
135F
143Y
188H
192R
Mutants
Replication capacity
CD4 down-modulation
HLA-A*02 down-modulation

B

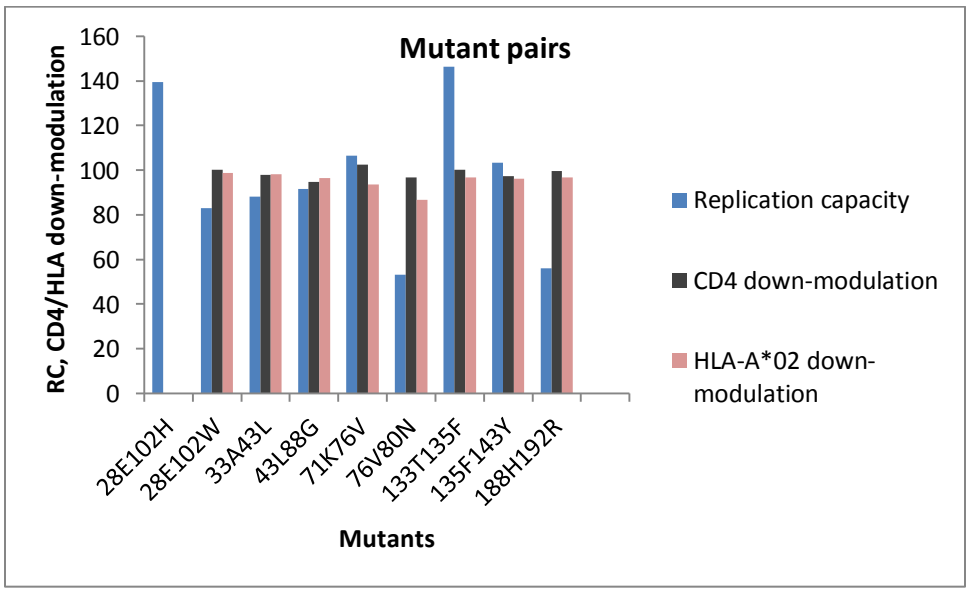
Mutant pairs
RC, CD4/HLA down-modulation
160
140
120
100
80
60
40
20
0
28E102H
28E102W
33A43L
43L88G
71K76V
76V80N
133T135F
135F143Y
188H192R
Mutants
Replication capacity
CD4 down-modulation
HLA-A*02 down-modulation

3.5.3 Variable amino acids at same codon

Mutants in this category were selected to test the ability of the Potts model to distinguish between, and assign E values accordingly, for different mutations at the same codon. The Potts model predicted higher fitness costs for 21E than 21K. However, the CD4 and HLA down-modulation capacities were highly similar for these two mutants and in fact, the replication capacity was lower for 21K which is not consistent with the Potts model predictions (Table 3.1 and Figure 3.9). The Potts model predicted a slightly higher energy cost for 57G compared to 57R (Table 3.1 and Figure 3.9). The CD4 down-modulation capacity of 57G was lower than that for 57R, which is consistent with the Potts model prediction; however the HLA down-modulation capacities and replication capacities of the two mutants were very similar (Table 3.1 and Figure 3.9). The Potts model predicted a higher energy cost for 80D than 80N. Consistent with this, the replication, CD4 and HLA down-modulation capacities of 80D were lower than that of 80N (Table 3.1 and Figure 3.9). The Potts model predicted higher fitness costs for 102W than 102H. However, the CD4 and HLA down-modulation capacities of these two mutants were similar and the replication capacity was actually lower for 102H which is not consistent with the Potts model predictions (Table 3.1 and Figure 3.9). The Potts model predicted higher fitness costs for 28E102W than 28E102H and in line with this, the replication capacity of 28E102W was lower compared to 28E102H (Table 3.1 and Figure 3.9). It should be noted that no statistics were performed on comparisons of mutants as repeated measurements of the same mutant or the wild-type and are not considered independent observations from a statistical perspective (161).

In summary, in three out of five instances the Potts model predictions were consistent with fitness/functional differences of different amino acid variants at the same codon.

Figure 3.9. Replication capacities as well as CD4 and HLA down-modulation capacities of mutants which fall into the category of variable amino acids at the same codon

The bars displayed in the graph are representative of the mean of replicates for the mutants replication capacities (blue) as well as CD4 down-modulation (grey) and HLA-A*02 down-modulation capacities (red).

In vitro replication capacities (RC) as well as Nef-mediated CD4 and HLA down-modulation capacities of the Nef mutants were normalised to that of the wild-type Nef (100 %)

The asterisk indicates missing data.

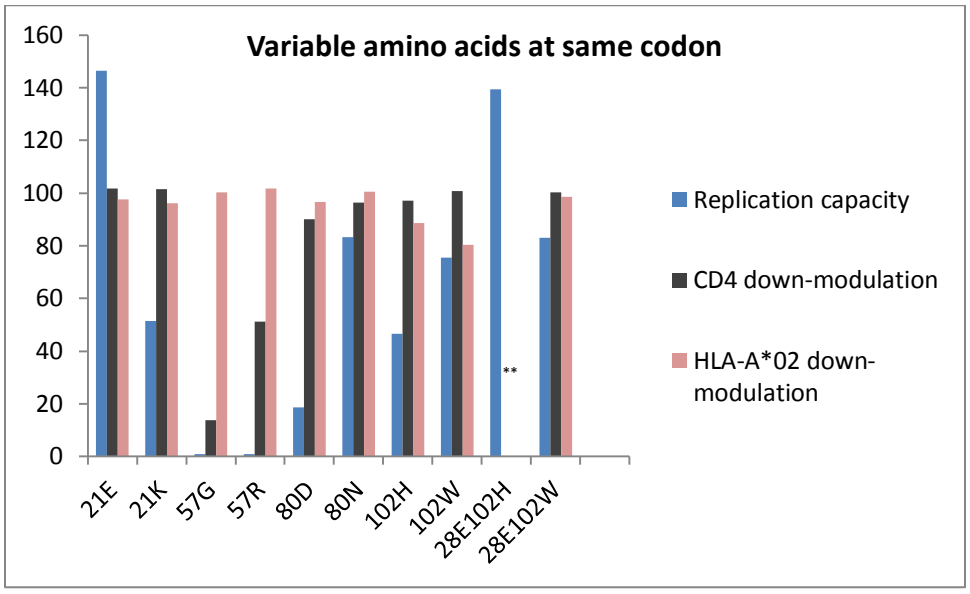
Variable amino acids at same codon
160
140
120
100
80
60
40
20
0
**
21E
21K
57G
57R
80D
80N
102H
102W
28E102H
28E102W
Replication capacity
CD4 down-modulation
HLA-A*02 down-modulation

3.5.4 Entropy versus models

Entropy has been used as a surrogate measure of viral fitness (98). It is expected that at residues with low entropy (high conservation), mutations will result in fitness costs. Therefore, we wanted to investigate whether the E values of the computational models were better predictors of viral fitness costs than the entropy of the residues at which the mutations occurred. The entropy of the relevant residues was calculated using published Nef sequences (107) and the entropy tool on the Los Alamos HIV sequence database (http://www.hiv.lanl.gov/content/sequence/ENTROPY/entropy.html). Considering only the single mutants (n = 19 for replication data and n = 20 for CD4 data), there was no correlation between the entropy of the residues at which the mutations occurred and replication capacity (Figure 3.10A, p = 0.3888) or CD4 down-modulation (Figure 3.10B, p = 0.0717), while Ising E values (but not Potts E values; data not shown) correlated significantly with replication capacity (Figure 3.10C, p = 0.0087) and CD4 down-modulation (Figure 3.10D, p = 0.0018) (Figure 3.10). As was the case for the model predictions (Section 3.3.2), entropy did not correlate with HLA-A*02 down-regulation ability (p = 0.0651) (data not shown).

Figure 3.10. Relationships between *in vitro* Nef-mediated replication capacities and CD4 down-modulation capacities of mutant Nef clones and entropy/Ising predicted E

(A) Graph showing no correlation ($r = 0.2097$, $p = 0.3888$) between replication capacities of mutant Nef clones and entropy.

(B) Graph showing no correlation ($r = 0.4111$, $p = 0.0717$) between CD4 down-modulation capacities of mutant Nef clones and entropy.

(C) Graph showing a significant negative correlation ($r = -0.5836$, $p = 0.0087$) between replication capacities of mutant Nef clones and E values predicted by the Ising model.

(D) Graph showing a significant negative correlation ($r = -0.6521$, $p = 0.0018$) between CD4 down-modulation capacities of mutant Nef clones and E values predicted by the Ising model.

In vitro replication capacities (RC) as well as Nef-mediated CD4 down-modulation capacities of the Nef mutants were normalised to that of the wild-type Nef (100 %)

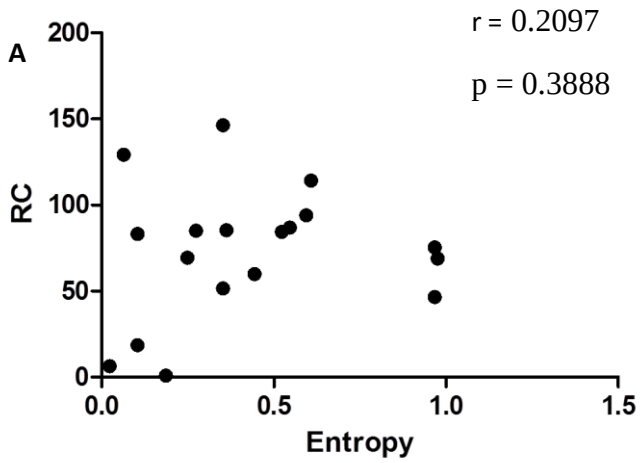
A
r = 0.2097
p = 0.3888
RC
Entropy
0
50
100
150
200
0.0
0.5
1.0
1.5

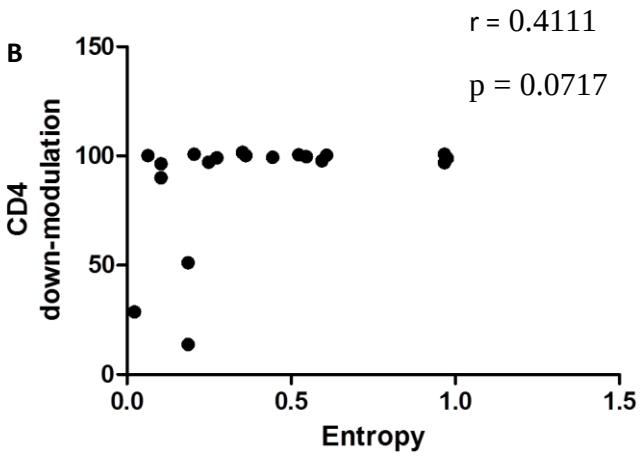
B
r = 0.4111
p = 0.0717
CD4
down-modulation
Entropy
0
50
100
150
0.0
0.5
1.0
1.5

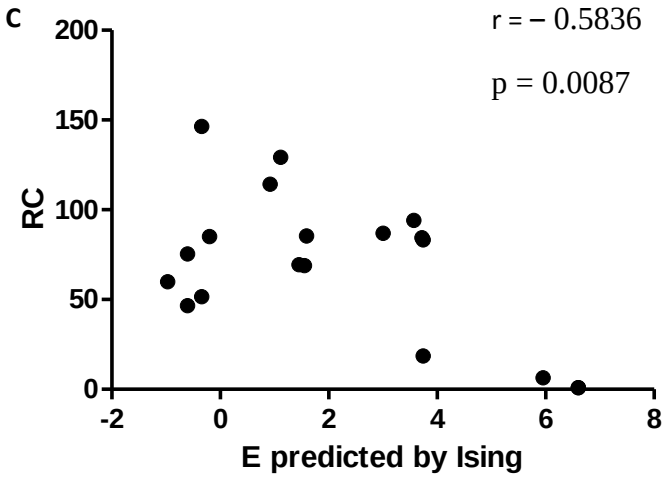
C
r = – 0.5836
p = 0.0087
RC
E predicted by Ising
0
50
100
150
200
-2
0
2
4
6
8

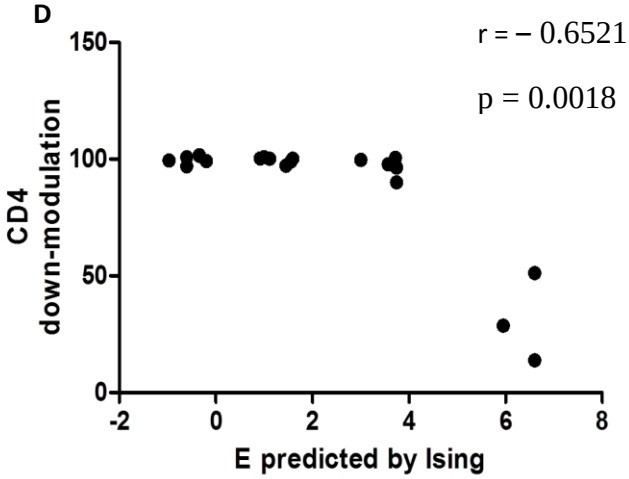
D
r = – 0.6521
p = 0.0018
CD4
down-modulation
E predicted by Ising
0
50
100
150
-2
0
2
4
6
8

CHAPTER 4

DISCUSSION

Due to the higkh mutability and constant immune evasion of the HIV-1 virus, an effective vaccine against the virus remains elusive (5, 85, 164). The HIV-1 Nef protein has been shown to contribute to HIV-1 pathogenesis and immune evasion (19, 39, 53, 78). Ising and Potts computational models have been designed with the ability of predicting the viral fitness landscape of the HIV- 1 Nef protein (49). These models, if validated, could potentially be used to identify vulnerable regions of Nef suitable for inclusion in a vaccine (49). The present study aimed to evaluate the accuracy of these computational models in predicting the fitness consequences of mutations in HIV-1 Nef, by measuring the Nef-driven replication capacities as well as CD4 and HLA down-modulation capacities of 32 different Nef mutants.

The E values (predicted fitness costs) predicted by both the Ising and Potts models correlated significantly with Nef-driven replication capacities and CD4 down-modulation capacities, but not HLA-A*02 down-modulation capacities, of the various Nef mutants. Mutations with higher E values tended to show lower Nef-driven replication as well as costs to CD4 down-modulation capacity. Thus the experimental data are in significant agreement with model predictions, indicating that the model was able to significantly predict fitness costs in the Nef protein. It is also important to note that the functional experimental outcomes for mutations within known functional motifs shown to affect CD4 and/or HLA down-modulation (Table 3.1) were consistent with what was previously documented in literature (Section 3.5.1) thus supporting the validity of our functional measurements. Furthermore, we determined that the Ising model of Nef fitness landscape is a better predictor of fitness costs in the Nef protein than simple entropy information.

The present study also aimed to compare the relative ability of the Ising and Potts models to predict the Nef fitness landscape. It was expected that the Potts model would be more reliable than the Ising model in predicting the fitness costs of mutations in highly mutable proteins such as Nef. The Ising model does not consider the identity of the mutant amino acid but defines the presence of mutations or the wild-type amino acid at each codon within each sequence in the MSA using a binary approximation: mutant amino acids are denoted as one and the wild-type amino acid is denoted as zero (49). While this is a good approximation for highly conserved proteins, such as Gag, it was expected that this may not be sufficient for highly variable proteins. The Potts model was developed to take specific amino acid mutations into account and assign E values according to the identified amino acid, rather than using the binary approximation (49). In the present study, it was observed that while the E values of both models correlated significantly with replication capacity and CD4 down-modulation, the correlations were stronger for Ising than Potts (Nef-driven replication capacity: $r = -0.5793$, $p = 0.0006$ for Ising and $r = -0.4118$, $p = 0.0213$ for Potts; CD4 down-modulation: $r = -0.5266$, $p = 0.0023$ for Ising and $r = -0.3781$, $p = 0.0360$ for Potts). This indicated that the Ising model was better at predicting fitness consequences of the selected mutations in HIV-1 Nef than the Potts model. A factor contributing to the better performance of the Ising model may be that in most cases the most common mutation at a particular codon was tested. The binary approximation of the Ising model is expected to be more representative of the most common mutations rather than rare ones. The difference between the expected and experimental outcomes might also be due to the Potts model allowing more amino acids per codon (for the ability to assign specific independent E values based on the particular amino acid at a specific codon) which could negatively interfere with the reliability of the model to infer interactions between different codons because pairs of rare

mutations are extremely infrequent. Essentially, considering multiple amino acids (while providing more information) may have negatively affected the performance and predictive ability of the model.

We selected mutants with variant amino acids to test the ability of the Potts model to accurately distinguish between, and assign E values accordingly, for different mutations at the same codon. It was observed that in three out of five instances the Potts model predictions were consistent with fitness/functional differences of different amino acid variants at the same codon. This indicates that the predictive ability of the Potts in this regard was not consistent. This could be further investigated by testing more mutants with variable amino acids at the same codon.

Previously, Ising and Potts computational models predicting the HIV-1 Gag fitness landscape were evaluated by measuring the replication capacities of 43 Gag mutants *in vitro* (105). The experimental data strongly correlated with predictions made by the Ising and Potts models for the Gag mutants ($r = -0.83$, $p = 3.76\times10^{-12}$ and $r = -0.73$, $p = 9.7\times10^{-9}$, respectively) (105). The correlations between predictions of both models and the replication capacities of Gag mutants were stronger than the correlations between model predictions and Nef-driven replication capacity ($r = -0.5793$, $p = 0.0006$ for Ising and $r = -0.4118$, $p = 0.0213$ for Potts) as well as between model predictions and Nef-mediated CD4 down-modulation ($r = -0.5266$, $p = 0.0023$ for Ising and $r = -0.3781$, $p = 0.0360$ for Potts). This indicated that both the Ising and the Potts models were more precise at predicting fitness consequences of mutations and mutation combinations in the highly conserved Gag protein than the variable Nef protein.

While the previous study testing the models of the HIV-1 Gag fitness landscape identified several pairs of HLA-associated mutations (likely CTL escape mutations) with high E values and substantial fitness costs, we did not identify HLA-associated mutations in Nef with substantial fitness costs in the present study. Only one HLA-associated mutant (80D) showed a notable reduction in replication capacity, and to our knowledge this mutation has not previously been associated with a fitness cost. The CD4 and HLA-A*02 down-modulation capacities of all the HLA-associated mutants were similar to that of the wild-type. This was despite the fact that the HLA-associated mutations and mutation pairs selected covered a range of E values, with 4 pairs having Ising E values > 5 as well as 2 single mutations and 5 mutation pairs having Potts E values > 5. (It was observed that substantial reductions in Nef-mediated CD4 down-regulation only occurred at E values >5). Our results indicate that it may be more difficult to identify observed escape mutations with a fitness cost in a highly variable protein such as Nef compared to the conserved Gag protein, which may suggest that to achieve significant functional impact in the Nef protein the virus will have to be forced down mutational escape pathways not commonly observed *in vivo*. Previous studies have shown that the fitness costs of escape mutations at conserved residues in Gag are greater than that in the more variable Env protein (149). Furthermore, another study showed that mutations in the conserved Gag p24 region tend to have greater fitness costs than mutations within the gp120 Env region even when only highly conserved amino acid sites are considered (99). However, there is some evidence that certain escape mutations in Nef could carry costs to viral fitness: HLA-B*35 associated mutations within a conserved region of Nef were shown to negatively affect virus replication and HLA-I down-modulation capacities (151). In another study which included 44 HLA-associated polymorphisms within Nef, it was reported that more than 50 % of the polymorphisms would

revert to the consensus following transmission to a HLA-mismatched recipient; which suggested that these polymorphisms come with fitness costs (2). Lastly, the number of HLA-associated polymorphisms (that were previously described to revert following transmission to a HLA-mismatched recipient (2)) was shown to correlate negatively with *in vitro* HLA down-modulation, indicating that that these polymorphisms do come with fitness costs (107).

We observed that the E values of both the Ising and Potts models correlated with replication capacity and CD4 down-modulation capacity but not HLA down-modulation capacity. This suggests that Nef-driven replication capacity and CD4 down-modulation may be more important functions *in vivo* than HLA down-modulation. In fact, previous studies suggest that CD4 down-modulation may be a more essential function of Nef *in vivo* than HLA down-modulation: it was previously shown that virus with eliminated HLA-down-modulation ability was still virulent (146), however when a Nef motif essential for CD4 down-modulation was disrupted (yet HLA down-regulation function was intact) SIV replication was greatly reduced (73). However, another possible reason for no correlation observed between E values and HLA-A*02 down-modulation capacities of the selected mutants could be that only two mutants displayed reduced HLA-A*02 down-modulation capacities. This likely reduced the ability to determine correlation between this parameter and the other parameters, i.e. E values and replication capacity, and could be further investigated in future studies by including more mutants that affect HLA-I down-modulation ability.

In the present study we observed that replication capacities of the Nef mutants correlated with CD4 down-modulation capacities but did not correlate with HLA-A*02 down-modulation capacities. The correlation between replication capacity and CD4 down-modulation was expected since Nef-mediated CD4 down-modulation directly enhances viral replication (Section 1.4.1) through an increase in the release of viral particles, as high levels of surface CD4 have been shown to interfere with the budding of virions (64, 139). When CD4 is down-modulated, Env sequestration into a CD4/Env complex which would result in impaired virion infectivity is avoided (125, 139). It was also expected that replication capacity would not correlate with HLA-A*02 down-modulation since HLA down-modulation enhances HIV-1 pathogenesis indirectly through immune evasion (53), and thus while it may indirectly enhance viral replication *in vivo*, it is unlikely to directly affect *in vitro* replicative ability.

There were some study limitations: the down-modulation of only HLA-A*02 was measured, however, in a previous study Nef-mediated HLA-A*02 down-modulation was highly correlated with HLA-B*07 down-modulation ($r=0.82$, $p<0.0001$) (106). Additionally, HLA down-modulation occurs through a sequence shared by the cytoplasmic tail of HLA-A and HLA-B molecules (89). Therefore, the ability of Nef to down-modulate HLA-A and HLA-B molecules may be generally represented by its ability to down-modulate HLA-A*02. The second limitation was that even though Nef is involved in many cellular functions (52), we focused only on replication capacity, CD4 down-modulation and HLA-I down-modulation. However, it was shown that these functions are important *in vivo* and do influence clinical outcome (73, 107, 124, 146). Lastly, we utilised PBMCs, since the presence of Nef is not essential for viral replication in many immortalized T cell lines (100), but PBMCs are highly variable between donors (18).

Nevertheless, we measured Nef-driven replication capacities using two different donors in this study and the measurements of the two donors were in good agreement ($r = 0.7780$, $p = <0.0001$; Section 3.2.1).

In conclusion, the experimental data was in significant agreement with both the Ising and the Potts models predictions of the fitness consequences of mutations in the Nef protein, and this was more accurate for the Ising model. However, the model predictions for Nef were not as accurate as for the highly conserved Gag protein. Nevertheless, the experimental data presented here support that computational modelling is a valid approach to rational immunogen design. The computational modelling approach is capable of identifying regions in the HIV-1 proteome which if targeted could force the virus down an undesirable pathway, which would lead to a substantial fitness cost to the virus, or could inhibit it from escaping immune responses due to the consequent fitness cost (49). It is also important to note that upon validation, the computational modelling approach is not restricted to HIV but could predict the fitness landscapes of other viruses and possibly cancers (49). The approach could therefore be used to direct immunogen design for a wide range of pathogens (49). Future studies are required to further validate models by identifying and designing HIV-1 vaccine immunogens to be tested in animal models.

REFERENCES

1. **Los Alamos National Laboratory**, HIV sequence database. Landmarks of the HIV-1 genome, HXB2, http://www.hiv.lanl.gov/content/sequence/HIV/MAP/landmark.html [Accessed: 2014]
2. **Adland, E., J. M. Carlson, P. Paioni, H. Kløverpris, R. Shapiro, A. Ogwu, L. Riddell, G. Luzzi, F. Chen, and T. Balachandran.** 2013. Nef-specific CD8+ T cell responses contribute to HIV-1 immune control. PloS one **8:**e73117.
3. **AIDSinfo.** 2005. The HIV Life Cycle. http://aidsinfo.nih.gov. [Accessed: 2014]
4. **Aiken, C., and D. Trono.** 1995. Nef stimulates human immunodeficiency virus type 1 proviral DNA synthesis. Journal of Virology **69:**5048-5056.
5. **Al-Jabri, A. A.** 2007. HIV/AIDS Vaccines: How long must humanity wait? Sultan Qaboos University Medical Journal **7:**193.
6. **Alimonti, J. B., T. B. Ball, and K. R. Fowke.** 2003. Mechanisms of CD4+ T lymphocyte cell death in human immunodeficiency virus infection and AIDS. Journal of General Virology **84:**1649-1661.
7. **Allen, T. M., and M. Altfeld.** 2008. Crippling HIV one mutation at a time. The Journal of Experimental Medicine **205:**1003-1007.
8. **Arhel, N.** 2010. Revisiting HIV-1 uncoating. Retrovirology **7:**96.
9. **Arhel, N. J., S. Souquere-Besse, S. Munier, P. Souque, S. Guadagnini, S. Rutherford, M.-C. Prévost, T. D. Allen, and P. Charneau.** 2007. HIV-1 DNA Flap formation promotes uncoating of the pre-integration complex at the nuclear pore. The EMBO Journal **26:**3025-3037.
10. **Barouch, D. H.** 2008. Challenges in the development of an HIV-1 vaccine. Nature **455:**613-619.
11. **Barré-Sinoussi, F., J.-C. Chermann, F. Rey, M. T. Nugeyre, S. Chamaret, J. Gruest, C. Dauguet, C. Axler-Blin, F. Vézinet-Brun, and C. Rouzioux.** 1983. Isolation of a T-lymphotropic retrovirus from a patient at risk for acquired immune deficiency syndrome (AIDS). Science **220:**868-871.

12. **Bevan, M. J., and T. J. Braciale.** 1995. Why can't cytotoxic T cells handle HIV? Proceedings of the National Academy of Sciences of the United States of America **92:**5765.

13. **Bleul, C. C., L. Wu, J. A. Hoxie, T. A. Springer, and C. R. Mackay.** 1997. The HIV coreceptors CXCR4 and CCR5 are differentially expressed and regulated on human T lymphocytes. Proceedings of the National Academy of Sciences **94:**1925-1930.

14. **Bor, J., A. J. Herbst, M.-L. Newell, and T. Bärnighausen.** 2013. Increases in adult life expectancy in rural South Africa: valuing the scale-up of HIV treatment. Science **339:**961-965.

15. **Brenchley, J. M., D. A. Price, and D. C. Douek.** 2006. HIV disease: fallout from a mucosal catastrophe? Nature Immunology **7:**235-239.

16. **Briggs, J. A., K. Grünewald, B. Glass, F. Förster, H.-G. Kräusslich, and S. D. Fuller.** 2006. The mechanism of HIV-1 core assembly: insights from three-dimensional reconstructions of authentic virions. Structure **14:**15-20.

17. **Brockman, M. A., A. Schneidewind, M. Lahaie, A. Schmidt, T. Miura, I. DeSouza, F. Ryvkin, C. A. Derdeyn, S. Allen, and E. Hunter.** 2007. Escape and compensation from early HLA-B57-mediated cytotoxic T-lymphocyte pressure on human immunodeficiency virus type 1 Gag alter capsid interactions with cyclophilin A. Journal of Virology **81:**12608-12618.

18. **Brockman, M. A., G. O. Tanzi, B. D. Walker, and T. M. Allen.** 2006. Use of a novel GFP reporter cell line to examine replication capacity of CXCR4-and CCR5-tropic HIV-1 by flow cytometry. Journal of Virological Methods **131:**134-142.

19. **Brumme, Z. L., M. John, J. M. Carlson, C. J. Brumme, D. Chan, M. A. Brockman, L. C. Swenson, I. Tao, S. Szeto, and P. Rosato.** 2009. HLA-associated immune escape pathways in HIV-1 subtype B Gag, Pol and Nef proteins. PloS one **4:**e6687.

20. **Buchacz, K., R. K. Baker, F. J. Palella Jr, J. S. Chmiel, K. A. Lichtenstein, R. M. Novak, K. C. Wood, and J. T. Brooks.** 2010. AIDS-defining opportunistic illnesses in US patients, 1994-2007: a cohort study. AIDS **24:**1549-1559.

21. **Buchbinder, S. P., D. V. Mehrotra, A. Duerr, D. W. Fitzgerald, R. Mogg, D. Li, P. B. Gilbert, J. R. Lama, M. Marmor, and C. del Rio.** 2008. Efficacy assessment of a cell-

mediated immunity HIV-1 vaccine (the Step Study): a double-blind, randomised, placebo-controlled, test-of-concept trial. The Lancet **372:**1881-1893.

22. **Carlson, J. M., C. J. Brumme, E. Martin, J. Listgarten, M. A. Brockman, A. Q. Le, C. Chui, L. A. Cotton, D. J. Knapp, and S. A. Riddler.** 2012. Correlates of protective cellular immunity revealed by analysis of population-level immune escape pathways in HIV-1. Journal of Virology**:**JVI. 01998-01912.
23. **Carlson, J. M., M. Schaefer, D. C. Monaco, R. Batorsky, D. T. Claiborne, J. Prince, M. J. Deymier, Z. S. Ende, N. R. Klatt, and C. E. DeZiel.** 2014. Selection bias at the heterosexual HIV-1 transmission bottleneck. Science **345:**1254031.
24. **Catalfamo, M., C. Wilhelm, L. Tcheung, M. Proschan, T. Friesen, J.-H. Park, J. Adelsberger, M. Baseler, F. Maldarelli, and R. Davey.** 2011. CD4 and CD8 T cell immune activation during chronic HIV infection: roles of homeostasis, HIV, type I IFN, and IL-7. The Journal of Immunology **186:**2106-2116.
25. **Cavrois, M., J. Neidleman, W. Yonemoto, D. Fenard, and W. C. Greene.** 2004. HIV-1 virion fusion assay: uncoating not required and no effect of Nef on fusion. Virology **328:**36-44.
26. **Cerboni, C., F. Neri, N. Casartelli, A. Zingoni, D. Cosman, P. Rossi, A. Santoni, and M. Doria.** 2007. Human immunodeficiency virus 1 Nef protein downmodulates the ligands of the activating receptor NKG2D and inhibits natural killer cell-mediated cytotoxicity. Journal of General Virology **88:**242-250.
27. **Chihara, T., M. Hashimoto, A. Osman, Y. Hiyoshi-Yoshidomi, I. Suzu, N. Chutiwitoonchai, M. Hiyoshi, S. Okada, and S. Suzu.** 2012. HIV-1 proteins preferentially activate anti-inflammatory M2-type macrophages. The Journal of Immunology **188:**3620-3627.
28. **Chopera, D. R., M. Mlotshwa, Z. Woodman, K. Mlisana, D. de Assis Rosa, D. P. Martin, S. A. Karim, C. M. Gray, and C. Williamson.** 2011. Virological and immunological factors associated with HIV-1 differential disease progression in HLA-B* 58: 01-positive individuals. Journal of Virology **85:**7070-7080.
29. **Chopera, D. R., J. K. Wright, M. A. Brockman, and Z. L. Brumme.** 2011. Immune-mediated attenuation of HIV-1. Future Virology **6:**917-928.

30. **Chu, C., and P. A. Selwyn.** 2010. Diagnosis and initial management of acute HIV infection. Am Fam Physician **81:**1239-1244.

31. **Çiledağ, A., and D. Karnak.** AIDS and Opportunistic Infections.

32. **Cimarelli, A., S. Sandin, S. Höglund, and J. Luban.** 2000. Basic residues in human immunodeficiency virus type 1 nucleocapsid promote virion assembly via interaction with RNA. Journal of Virology **74:**3046-3057.

33. **Cohen, G. B., R. T. Gandhi, D. M. Davis, O. Mandelboim, B. K. Chen, J. L. Strominger, and D. Baltimore.** 1999. The selective downregulation of class I major histocompatibility complex proteins by HIV-1 protects HIV-infected cells from NK cells. Immunity **10:**661-671.

34. **Cohen, M. S., and C. L. Gay.** 2010. Treatment to prevent transmission of HIV-1. Clinical Infectious Diseases **50:**S85-S95.

35. **Cohen, M. S., C. L. Gay, M. P. Busch, and F. M. Hecht.** 2010. The detection of acute HIV infection. Journal of Infectious Diseases **202:**S270-S277.

36. **Cohen, M. S., N. Hellmann, J. A. Levy, K. DeCock, and J. Lange.** 2008. The spread, treatment, and prevention of HIV-1: evolution of a global pandemic. The Journal of Clinical Investigation **118:**1244.

37. **Coleman, C. M., and L. Wu.** 2009. HIV interactions with monocytes and dendritic cells: viral latency and reservoirs. Retrovirology **6:**51.

38. **Costa, L. J., L. M. Mendonça, and T. L. Sampaio.** Functions of the Lentiviral Accessory Protein Nef During the Distinct Steps of HIV and SIV Replication Cycle.

39. **Crawford, H., J. G. Prado, A. Leslie, S. Hué, I. Honeyborne, S. Reddy, M. van der Stok, Z. Mncube, C. Brander, and C. Rousseau.** 2007. Compensatory mutation partially restores fitness and delays reversion of escape mutation within the immunodominant HLA-B* 5703-restricted Gag epitope in chronic human immunodeficiency virus type 1 infection. Journal of Virology **81:**8346-8351.

40. **Dahirel, V., K. Shekhar, F. Pereyra, T. Miura, M. Artyomov, S. Talsania, T. M. Allen, M. Altfeld, M. Carrington, and D. J. Irvine.** 2011. Coordinate linkage of HIV evolution reveals regions of immunological vulnerability. Proceedings of the National Academy of Sciences **108:**11530-11535.

41. **Das, S. R., and S. Jameel.** 2005. Biology of the HIV Nef protein. Indian J Med Res **121:**315-332.

42. **De Clercq, E.** 2009. Anti-HIV drugs: 25 compounds approved within 25 years after the discovery of HIV. International Journal of Antimicrobial Agents **33:**307-320.

43. **Doms, R. W., and D. Trono.** 2000. The plasma membrane as a combat zone in the HIV battlefield. Genes & Development **14:**2677-2688.

44. **Douek, D. C., L. J. Picker, and R. A. Koup.** 2003. T Cell Dynamics in HIV-1 Infection*. Annual Review of Immunology **21:**265-304.

45. **Emerman, M., and M. H. Malim.** 1998. HIV-1 regulatory/accessory genes: keys to unraveling viral and host cell biology. Science **280:**1880-1884.

46. **Fauci, A. S., and H. Clifford Lane.** 1998. Human immunodeficiency virus (HIV) disease: AIDS and related disorders. Harrisons Principles of Internal Medicine**:**1791-1855.

47. **Fauci, A. S., and H. C. Lane.** 2005. Human Immunodeficiency Virus Disease: AIDS and Related Disorders., Kasper, D.L., Braunwald, E., Fauci, A.S., Hauser, S.L., Longo, D.L., Jameson, J.L., eds. Harrison's Principles of Internal Medicine, 16th ed, New York: McGraw-Hill Professional.

48. **Fauci, A. S., G. Pantaleo, S. Stanley, and D. Weissman.** 1996. Immunopathogenic mechanisms of HIV infection. Annals of Internal Medicine **124:**654-663.

49. **Ferguson, A. L., J. K. Mann, S. Omarjee, T. Ndung'u, B. D. Walker, and A. K. Chakraborty.** 2013. Translating HIV Sequences into Quantitative Fitness Landscapes Predicts Viral Vulnerabilities for Rational Immunogen Design. Immunity **38:**606-617.

50. **Finzi, D., J. Blankson, J. D. Siliciano, J. B. Margolick, K. Chadwick, T. Pierson, K. Smith, J. Lisziewicz, F. Lori, and C. Flexner.** 1999. Latent infection of CD4+ T cells provides a mechanism for lifelong persistence of HIV-1, even in patients on effective combination therapy. Nature Medicine **5:**512-517.

51. **Foster, J., and J. V. Garcia.** 2008. HIV-1 Nef: at the crossroads. Retrovirology **5:**84.

52. **Foster, J. L., S. J. Denial, B. R. Temple, and J. V. Garcia.** 2011. Mechanisms of HIV-1 Nef function and intracellular signaling. Journal of Neuroimmune Pharmacology **6:**230-246.

53. **Foster, J. L., and J. V. Garcia.** 2008. HIV-1 Nef: at the crossroads. Retrovirology **5:**84.

54. **Frankel, A. D., and J. A. Young.** 1998. HIV-1: fifteen proteins and an RNA. Annual review of Biochemistry **67:**1-25.

55. **Freed, E. O.** 2001. HIV-1 replication. Somatic cell and Molecular Genetics **26:**13-33.

56. **Fujiwara, M., J. Tanuma, H. Koizumi, Y. Kawashima, K. Honda, S. Mastuoka-Aizawa, S. Dohki, S. Oka, and M. Takiguchi.** 2008. Different abilities of escape mutant-specific cytotoxic T cells to suppress replication of escape mutant and wild-type human immunodeficiency virus type 1 in new hosts. Journal of Virology **82:**138-147.

57. **Gaardbo, J. C., H. J. Hartling, J. Gerstoft, and S. D. Nielsen.** 2012. Thirty Years with HIV Infection—Nonprogression Is Still Puzzling: Lessons to Be Learned from Controllers and Long-Term Nonprogressors. AIDS Research and Treatment **2012**.

58. **Ganser, B. K., S. Li, V. Y. Klishko, J. T. Finch, and W. I. Sundquist.** 1999. Assembly and analysis of conical models for the HIV-1 core. Science **283:**80-83.

59. **Geleziunas, R., W. Xu, K. Takeda, H. Ichijo, and W. C. Greene.** 2001. HIV-1 Nef inhibits ASK1-dependent death signalling providing a potential mechanism for protecting the infected host cell. Nature **410:**834-838.

60. **Geyer, M., O. T. Fackler, and B. M. Peterlin.** 2001. Structure–function relationships in HIV-1 Nef. EMBO reports **2:**580-585.

61. **Gomez, C., and T. J. Hope.** 2005. The ins and outs of HIV replication. Cellular Microbiology **7:**621-626.

62. **Goonetilleke, N., M. K. Liu, J. F. Salazar-Gonzalez, G. Ferrari, E. Giorgi, V. V. Ganusov, B. F. Keele, G. H. Learn, E. L. Turnbull, and M. G. Salazar.** 2009. The first T cell response to transmitted/founder virus contributes to the control of acute viremia in HIV-1 infection. The Journal of Experimental Medicine **206:**1253-1272.

63. **Götte, M., X. Li, and M. A. Wainberg.** 1999. HIV-1 reverse transcription: A brief overview focused on structure–function relationships among molecules involved in initiation of the reaction. Archives of Biochemistry and Biophysics **365:**199-210.

64. **Greenway, A. L., G. Holloway, D. A. McPhee, P. Ellis, A. Cornall, and M. Lidman.** 2003. HIV-1 Nef control of cell signalling molecules: multiple strategies to promote virus replication. Journal of Biosciences **28:**323-335.

65. **Gross, I., H. Hohenberg, C. Huckhagel, and H.-G. Kräusslich.** 1998. N-terminal extension of human immunodeficiency virus capsid protein converts the in vitro

assembly phenotype from tubular to spherical particles. Journal of Virology **72:**4798-4810.

66. **Grossman, Z., M. Meier-Schellersheim, A. E. Sousa, R. M. Victorino, and W. E. Paul.** 2002. CD 4+ T-cell depletion in HIV infection: are we closer to understanding the cause? Nature Medicine **8:**319-323.
67. **Grzesiek, S., S. J. Stahl, P. T. Wingfield, and A. Bax.** 1996. The CD4 determinant for downregulation by HIV-1 Nef directly binds to Nef. Mapping of the Nef binding surface by NMR. Biochemistry **35:**10256-10261.
68. **Hansasuta, P., and S. L. Rowland-Jones.** 2001. HIV-1 transmission and acute HIV-1 infection. British Medical Bulletin **58:**109-127.
69. **Hayes, R., S. Kapiga, N. Padian, S. McCormack, and J. Wasserheit.** 2010. HIV prevention research: taking stock and the way forward. AIDS (London, England) **24:**S81.
70. **Hernandez-Vargas, E. A., and R. H. Middleton.** 2012. Modelling the three stages in HIV infection. Journal of Theoretical Biology.
71. **Hu WS, and H. SH.** 2012. HIV-1 reverse transcription. Cold Spring Harbor Perspectives in Medicine **2**.
72. **Huang, C.-c., M. Tang, M.-Y. Zhang, S. Majeed, E. Montabana, R. L. Stanfield, D. S. Dimitrov, B. Korber, J. Sodroski, and I. A. Wilson.** 2005. Structure of a V3-containing HIV-1 gp120 core. Science **310:**1025-1028.
73. **Iafrate, A. J., S. Carl, S. Bronson, C. Stahl-Hennig, T. Swigut, J. Skowronski, and F. Kirchhoff.** 2000. Disrupting surfaces of nef required for downregulation of CD4 and for enhancement of virion infectivity attenuates simian immunodeficiency virus replication in vivo. Journal of Virology **74(21):**9836-9844.
74. **Jamieson, B. D., G. M. Aldrovandi, V. Planelles, J. Jowett, L. Gao, L. M. Bloch, I. Chen, and J. A. Zack.** 1994. Requirement of human immunodeficiency virus type 1 nef for in vivo replication and pathogenicity. Journal of Virology **68:**3478-3485.
75. **Jia, B., R. Serra-Moreno, W. Neidermyer Jr, A. Rahmberg, J. Mackey, I. B. Fofana, W. E. Johnson, S. Westmoreland, and D. T. Evans.** 2009. Species-specific activity of SIV Nef and HIV-1 Vpu in overcoming restriction by tetherin/BST2. PLoS pathogens **5:**e1000429.

76. **Kassutto, S., and E. S. Rosenberg.** 2004. Primary HIV type 1 infection. Clinical Infectious Diseases **38:**1447-1453.

77. **Kemal, K. S., T. Beattie, T. Dong, B. Weiser, R. Kaul, C. Kuiken, J. Sutton, D. Lang, H. Yang, and Y. C. Peng.** 2008. Transition from long-term nonprogression to HIV-1 disease associated with escape from cellular immune control. JAIDS Journal of Acquired Immune Deficiency Syndromes **48:**119-126.

78. **Kestier, H. W., D. J. Ringler, K. Mori, D. L. Panicali, P. K. Sehgal, M. D. Daniel, and R. C. Desrosiers.** 1991. Importance of the< i> nef</i> gene for maintenance of high virus loads and for development of AIDS. Cell **65:**651-662.

79. **Kim, J.-H., R. L. Riolo, and J. S. Koopman.** 2010. HIV transmission by stage of infection and pattern of sexual partnerships. Epidemiology (Cambridge, Mass.) **21:**676.

80. **Kirchhoff, F.** 2010. Immune evasion and counteraction of restriction factors by HIV-1 and other primate lentiviruses. Cell host & Microbe **8:**55-67.

81. **Kirchhoff, F., T. C. Greenough, D. B. Brettler, J. L. Sullivan, and R. C. Desrosiers.** 1995. Absence of intact nef sequences in a long-term survivor with nonprogressive HIV-1 infection. New England Journal of Medicine **332:**228-232.

82. **Koppensteiner, H., R. Brack-Werner, and M. Schindler.** 2012. Macrophages and their relevance in Human Immunodeficiency Virus Type I infection. Retrovirology **9:**1-11.

83. **Koup, R., J. T. Safrit, Y. Cao, C. A. Andrews, G. McLeod, W. Borkowsky, C. Farthing, and D. D. Ho.** 1994. Temporal association of cellular immune responses with the initial control of viremia in primary human immunodeficiency virus type 1 syndrome. Journal of Virology **68:**4650-4655.

84. **Kuznetsov, Y. G., J. Victoria, W. Robinson, and A. McPherson.** 2003. Atomic force microscopy investigation of human immunodeficiency virus (HIV) and HIV-infected lymphocytes. Journal of Virology **77:**11896-11909.

85. **Kwong, P. D., J. R. Mascola, and G. J. Nabel.** 2012. The changing face of HIV vaccine research. Journal of the International AIDS Society **15**.

86. **Kwong, P. D., R. Wyatt, J. Robinson, R. W. Sweet, J. Sodroski, and W. A. Hendrickson.** 1998. Structure of an HIV gp120 envelope glycoprotein in complex with the CD4 receptor and a neutralizing human antibody. Nature **393:**648-659.

87. **Lamers, S. L., G. B. Fogel, E. J. Singer, M. Salemi, D. J. Nolan, L. C. Huysentruyt, and M. S. McGrath.** 2012. HIV-1 Nef in Macrophage-Mediated Disease Pathogenesis. International Reviews of Immunology **31:**432-450.

88. **Lanman, J., T. T. Lam, M. R. Emmett, A. G. Marshall, M. Sakalian, and P. E. Prevelige.** 2004. Key interactions in HIV-1 maturation identified by hydrogen-deuterium exchange. Nature Structural & Molecular Biology **11:**676-677.

89. **Le Gall, S., L. Erdtmann, S. Benichou, C. Berlioz-Torrent, L. Liu, R. Benarous, J.-M. Heard, and O. Schwartz.** 1998. Nef interacts with the μ subunit of clathrin adaptor complexes and reveals a cryptic sorting signal in MHC I molecules. Immunity **8:**483-495.

90. **Lenassi, M., G. Cagney, M. Liao, T. Vaupotič, K. Bartholomeeusen, Y. Cheng, N. J. Krogan, A. Plemenitaš, and B. M. Peterlin.** 2010. HIV Nef is secreted in exosomes and triggers apoptosis in bystander CD4+ T cells. Traffic **11:**110-122.

91. **Leonard, J. A., T. Filzen, C. C. Carter, M. Schaefer, and K. L. Collins.** 2011. HIV-1 Nef disrupts intracellular trafficking of major histocompatibility complex class I, CD4, CD8, and CD28 by distinct pathways that share common elements. Journal of Virology **85:**6867-6881.

92. **Leslie, A., D. A. Price, P. Mkhize, K. Bishop, A. Rathod, C. Day, H. Crawford, I. Honeyborne, T. E. Asher, and G. Luzzi.** 2006. Differential selection pressure exerted on HIV by CTL targeting identical epitopes but restricted by distinct HLA alleles from the same HLA supertype. The Journal of Immunology **177:**4699-4708.

93. **Letvin, N. L., and B. D. Walker.** 2003. Immunopathogenesis and immunotherapy in AIDS virus infections. Nature Medicine **9:**861-866.

94. **Leung, K., J.-O. Kim, L. Ganesh, J. Kabat, O. Schwartz, and G. J. Nabel.** 2008. HIV-1 assembly: viral glycoproteins segregate quantally to lipid rafts that associate individually with HIV-1 capsids and virions. Cell host & Microbe **3:**285-292.

95. **Lewin, S. R., V. A. Evans, J. H. Elliott, B. Spire, and N. Chomont.** 2011. Finding a cure for HIV: will it ever be achievable? Journal of the International AIDS Society **14:**4.

96. **Li, C., A. Wen, B. Shen, J. Lu, Y. Huang, and Y. Chang.** 2011. FastCloning: a highly simplified, purification-free, sequence-and ligation-independent PCR cloning method. BMC Biotechnology **11:**92.

97. **Li, M., and R. Craigie.** 2005. Processing of viral DNA ends channels the HIV-1 integration reaction to concerted integration. Journal of Biological Chemistry **280:**29334-29339.

98. **Liu, M. K., N. Hawkins, A. J. Ritchie, V. V. Ganusov, V. Whale, S. Brackenridge, H. Li, J. W. Pavlicek, F. Cai, and M. Rose-Abrahams.** 2013. Vertical T cell immunodominance and epitope entropy determine HIV-1 escape. The Journal of Clinical Investigation **123:**380.

99. **Liu, Y., U. Rao, J. McClure, P. Konopa, S. Manocheewa, M. Kim, L. Chen, R. M. Troyer, D. M. Tebit, and S. Holte.** 2014. Impact of mutations in highly conserved amino acids of the HIV-1 Gag-p24 and Env-gp120 proteins on viral replication in different genetic backgrounds. PloS one **9:**e94240.

100. **Lundquist, C. A., M. Tobiume, J. Zhou, D. Unutmaz, and C. Aiken.** 2002. Nef-mediated downregulation of CD4 enhances human immunodeficiency virus type 1 replication in primary T lymphocytes. Journal of Virology **76:**4625-4633.

101. **MacLeod, M. K., J. W. Kappler, and P. Marrack.** 2010. Memory CD4 T cells: generation, reactivation and re-assignment. Immunology **130:**10-15.

102. **Malim, M. H., and P. D. Bieniasz.** 2012. HIV restriction factors and mechanisms of evasion. Cold Spring Harbor Perspectives in Medicine **2**.

103. **Malim, M. H., and M. Emerman.** 2008. HIV-1 accessory proteins—ensuring viral survival in a hostile environment. Cell host & Microbe **3:**388-398.

104. **Mangasarian, A., V. Piguet, J.-K. Wang, Y.-L. Chen, and D. Trono.** 1999. Nef-induced CD4 and major histocompatibility complex class I (MHC-I) down-regulation are governed by distinct determinants: N-terminal alpha helix and proline repeat of Nef selectively regulate MHC-I trafficking. Journal of Virology **73:**1964-1973.

105. **Mann, J. K., J. P. Barton, A. L. Ferguson, S. Omarjee, B. D. Walker, A. Chakraborty, and T. Ndung'u.** 2014. The fitness landscape of HIV-1 gag: advanced modeling approaches and validation of model predictions by in vitro testing. PLoS Computational Biology **10:**e1003776.

106. **Mann, J. K., H. Byakwaga, X. T. Kuang, A. Q. Le, C. J. Brumme, P. Mwimanzi, S. Omarjee, E. Martin, G. Q. Lee, and B. Baraki.** 2013. Ability of HIV-1 Nef to downregulate CD4 and HLA class I differs among viral subtypes. Retrovirology **10:**100.

107. **Mann, J. K., D. Chopera, S. Omarjee, X. T. Kuang, A. Q. Le, G. Anmole, R. Danroth, P. Mwimanzi, T. Reddy, and J. Carlson.** 2014. Nef-mediated down-regulation of CD4 and HLA class I in HIV-1 subtype C infection: Association with disease progression and influence of immune pressure. Virology **468:**214-225.

108. **Markosyan, R. M., F. S. Cohen, and G. B. Melikyan.** 2003. HIV-1 envelope proteins complete their folding into six-helix bundles immediately after fusion pore formation. Molecular Biology of the Cell **14:**926-938.

109. **Martinez-Picado, J., J. G. Prado, E. E. Fry, K. Pfafferott, A. Leslie, S. Chetty, C. Thobakgale, I. Honeyborne, H. Crawford, and P. Matthews.** 2006. Fitness cost of escape mutations in p24 Gag in association with control of human immunodeficiency virus type 1. Journal of Virology **80:**3617-3623.

110. **Matthews, S., P. Barlow, J. Boyd, G. Barton, R. Russell, H. Mills, M. Cunningham, N. Meyers, N. Burns, and N. Clark.** 1994. Structural similarity between the p17 matrix protein of HIV-1 and interferon-g. Nature **370:**666-668.

111. **Mavilio, D., J. Benjamin, M. Daucher, G. Lombardo, S. Kottilil, M. A. Planta, E. Marcenaro, C. Bottino, L. Moretta, and A. Moretta.** 2003. Natural killer cells in HIV-1 infection: dichotomous effects of viremia on inhibitory and activating receptors and their functional correlates. Proceedings of the National Academy of Sciences **100:**15011-15016.

112. **McElrath, M. J.** 2010. Immune responses to HIV vaccines and potential impact on control of acute HIV-1 infection. Journal of Infectious Diseases **202:**S323-S326.

113. **McMichael, A. J., P. Borrow, G. D. Tomaras, N. Goonetilleke, and B. F. Haynes.** 2009. The immune response during acute HIV-1 infection: clues for vaccine development. Nature Reviews Immunology **10:**11-23.

114. **Mebatsion, T., S. Finke, F. Weiland, and K.-K. Conzelmann.** 1997. A CXCR4/CD4 pseudotype rhabdovirus that selectively infects HIV-1 envelope protein-expressing cells. Cell **90:**841-847.

115. **Melikyan, G. B., R. M. Markosyan, H. Hemmati, M. K. Delmedico, D. M. Lambert, and F. S. Cohen.** 2000. Evidence that the transition of HIV-1 gp41 into a six-helix bundle, not the bundle configuration, induces membrane fusion. The Journal of Cell Biology **151:**413-424.

116. **Mlisana, K.** HIV Vaccine development: Challenges and Progress.

117. **Mogensen, T. H., J. Melchjorsen, C. S. Larsen, and S. R. Paludan.** 2010. Review Innate immune recognition and activation during HIV infection.

118. **Montefiori, D. C., C. Karnasuta, Y. Huang, H. Ahmed, P. Gilbert, M. S. de Souza, R. McLinden, S. Tovanabutra, A. Laurence-Chenine, and E. Sanders-Buell.** 2012. Magnitude and breadth of the neutralizing antibody response in the RV144 and Vax003 HIV-1 vaccine efficacy trials. Journal of Infectious Diseases **206:**431-441.

119. **Moris, A., A. Pajot, F. Blanchet, F. Guivel-Benhassine, M. Salcedo, and O. Schwartz.** 2006. Dendritic cells and HIV-specific CD4+ T cells: HIV antigen presentation, T-cell activation, and viral transfer. Blood **108:**1643-1651.

120. **Mougel, M., A. Cimarelli, and J.-L. Darlix.** 2010. Implications of the nucleocapsid and the microenvironment in retroviral reverse transcription. Viruses **2:**939-960.

121. **Muriaux, D., and J.-L. Darlix.** 2010. Properties and functions of the nucleocapsid protein in virus assembly. RNA Biology **7:**744-753.

122. **Mwimanzi, P., Z. Hasan, R. Hassan, S. Suzu, M. Takiguchi, and T. Ueno.** 2011. Effects of naturally-arising HIV Nef mutations on cytotoxic T lymphocyte recognition and Nef's functionality in primary macrophages. Retrovirology **8:**50.

123. **Mwimanzi, P., T. J. Markle, E. Martin, Y. Ogata, X. T. Kuang, M. Tokunaga, M. Mahiti, F. Pereyra, T. Miura, and B. D. Walker.** 2013. Attenuation of multiple Nef functions in HIV-1 elite controllers. Retrovirology **10:**1.

124. **Mwimanzi, P., T. J. Markle, T. Ueno, and M. A. Brockman.** 2012. Human Leukocyte Antigen (HLA) Class I Down-Regulation by Human Immunodeficiency Virus Type 1 Negative Factor (HIV-1 Nef): What Might We Learn From Natural Sequence Variants? Viruses **4:**1711-1730.

125. **Neri, F., G. Giolo, M. Potestà, S. Petrini, and M. Doria.** 2011. CD4 downregulation by the human immunodeficiency virus type 1 Nef protein is dispensable for optimal output and functionality of viral particles in primary T cells. Journal of General Virology **92:**141-150.

126. **Nielsen, M. H., F. S. Pedersen, and J. Kjems.** 2005. Molecular strategies to inhibit HIV-1 replication. Retrovirology **2:**10.

127. **O'Doherty, U., W. J. Swiggard, and M. H. Malim.** 2000. Human immunodeficiency virus type 1 spinoculation enhances infection through virus binding. Journal of Virology **74:**10074-10080.

128. **Olivieri, K. C., J. Mukerji, and D. Gabuzda.** 2011. Nef-mediated enhancement of cellular activation and human immunodeficiency virus type 1 replication in primary T cells is dependent on association with p21-activated kinase 2. Retrovirology **8:**1-17.

129. **Ono, A., and E. O. Freed.** 2001. Plasma membrane rafts play a critical role in HIV-1 assembly and release. Proceedings of the National Academy of Sciences **98:**13925-13930.

130. **Pace, M. J., E. H. Graf, L. M. Agosto, A. M. Mexas, F. Male, T. Brady, F. D. Bushman, and U. O'Doherty.** 2012. Directly infected resting CD4+ T cells can produce HIV Gag without spreading infection in a model of HIV latency. PLoS Pathog **8:**e1002818.

131. **Pancino, G., K. Yarbrough, V. Arnold, and D. Scott-Algara.** 2008. Natural Killer Cells â An Underestimated Defence Against HIV?

132. **Pantaleo, G., and A. S. Fauci.** 1995. New concepts in the immunopathogenesis of HIV infection. Annual review of Immunology **13:**487-512.

133. **Piguet, V., and D. Trono.** 1999. The Nef protein of primate lentiviruses. Reviews in Medical Virology **9:**111-120.

134. **Piguet, V., L. Wan, C. Borel, A. Mangasarian, N. Demaurex, G. Thomas, and D. Trono.** 2000. HIV-1 Nef protein binds to the cellular protein PACS-1 to downregulate class I major histocompatibility complexes. Nature Cell Biology **2:**163-167.

135. **Price, D. A., P. J. Goulder, P. Klenerman, A. K. Sewell, P. J. Easterbrook, M. Troop, C. R. Bangham, and R. E. Phillips.** 1997. Positive selection of HIV-1 cytotoxic T lymphocyte escape variants during primary infection. Proceedings of the National Academy of Sciences **94:**1890-1895.

136. **Quiñones-Mateu, M. E., S. C. Ball, A. J. Marozsan, V. S. Torre, J. L. Albright, G. Vanham, G. van der Groen, R. L. Colebunders, and E. J. Arts.** 2000. A dual infection/competition assay shows a correlation between ex vivo human immunodeficiency virus type 1 fitness and disease progression. Journal of Virology **74:**9222-9233.

137. **Rerks-Ngarm, S., P. Pitisuttithum, S. Nitayaphan, J. Kaewkungwal, J. Chiu, R. Paris, N. Premsri, C. Namwat, M. de Souza, and E. Adams.** 2009. Vaccination with ALVAC and AIDSVAX to prevent HIV-1 infection in Thailand. New England Journal of Medicine **361:**2209-2220.

138. **Roebuck, K., and M. Saifuddin.** 1999. Regulation of HIV-1 transcription. Gene expression **8:**67.

139. **Ross, T. M., A. E. Oran, and B. R. Cullen.** 1999. Inhibition of HIV-1 progeny virion release by cell-surface CD4 is relieved by expression of the viral Nef protein. Current Biology **9:**613-621.

140. **Sauce, D., C. Elbim, and V. Appay.** 2013. Monitoring cellular immune markers in HIV infection: from activation to exhaustion. Current Opinion in HIV and AIDS **8:**125-131.

141. **Schaefer, M. R., E. R. Wonderlich, J. F. Roeth, J. A. Leonard, and K. L. Collins.** 2008. HIV-1 Nef targets MHC-I and CD4 for degradation via a final common β-COP–dependent pathway in T cells. PLoS pathogens **4:**e1000131.

142. **Seelamgari, A., A. Maddukuri, R. Berro, C. de la Fuente, K. Kehn, L. Deng, S. Dadgar, M. E. Bottazzi, E. Ghedin, and A. Pumfery.** 2004. Role of viral regulatory and accessory proteins in HIV-1 replication. Frontiers in bioscience: A Journal and Virtual Library **9:**2388-2413.

143. **Sharma, G., G. Kaur, and N. Mehra.** 2011. Genetic correlates influencing immunopathogenesis of HIV infection. The Indian Journal of Medical Research **134:**749.

144. **Shulman, N., A. R. Zolopa, D. Passaro, R. W. Shafer, W. Huang, D. Katzenstein, D. M. Israelski, N. Hellmann, C. Petropoulos, and J. Whitcomb.** 2001. Phenotypic hypersusceptibility to non-nucleoside reverse transcriptase inhibitors in treatment-experienced HIV-infected patients: impact on virological response to efavirenz-based therapy. Aids **15:**1125-1132.

145. **Stevenson, M.** 2003. HIV-1 pathogenesis. Nature Medicine **9:**853-860.

146. **Swigut, T., L. Alexander, J. Morgan, J. Lifson, K. G. Mansfield, S. Lang, R. P. Johnson, J. Skowronski, and R. Desrosiers.** 2004. Impact of Nef-mediated downregulation of major histocompatibility complex class I on immune response to simian immunodeficiency virus. Journal of Virology **78(23):**13335-13344.

147. **Swingler, S., B. Brichacek, J.-M. Jacque, C. Ulich, J. Zhou, and M. Stevenson.** 2003. HIV-1 Nef intersects the macrophage CD40L signalling pathway to promote resting-cell infection. Nature **424:**213-219.

148. **Thompson, M. A., J. A. Aberg, P. Cahn, J. S. Montaner, G. Rizzardini, A. Telenti, J. M. Gatell, H. F. Günthard, S. M. Hammer, and M. S. Hirsch.** 2010. Antiretroviral treatment of adult HIV infection. JAMA: The Journal of the American Medical Association **304:**321-333.

149. **Troyer, R. M., J. McNevin, Y. Liu, S. C. Zhang, R. W. Krizan, A. Abraha, D. M. Tebit, H. Zhao, S. Avila, and M. A. Lobritz.** 2009. Variable fitness impact of HIV-1 escape mutations to cytotoxic T lymphocyte (CTL) response. PLoS pathogens **5:**e1000365.

150. **Ueno, T., Y. Idegami, C. Motozono, S. Oka, and M. Takiguchi.** 2007. Altering effects of antigenic variations in HIV-1 on antiviral effectiveness of HIV-specific CTLs. The Journal of Immunology **178:**5513-5523.

151. **Ueno, T., C. Motozono, S. Dohki, P. Mwimanzi, S. Rauch, O. T. Fackler, S. Oka, and M. Takiguchi.** 2008. CTL-mediated selective pressure influences dynamic evolution and pathogenic functions of HIV-1 Nef. The Journal of Immunology **180:**1107-1116.

152. **Van Maele, B., and Z. Debyser.** 2005. HIV-1 integration: an interplay between HIV-1 integrase, cellular and viral proteins. AIDS Rev **7:**26-43.

153. **Watts, J. M., K. K. Dang, R. J. Gorelick, C. W. Leonard, J. W. Bess Jr, R. Swanstrom, C. L. Burch, and K. M. Weeks.** 2009. Architecture and secondary structure of an entire HIV-1 RNA genome. Nature **460:**711-716.

154. **Weber, J.** 2001. The pathogenesis of HIV-1 infection. British Medical Bulletin **58:**61-72.

155. **Wei, X., J. M. Decker, S. Wang, H. Hui, J. C. Kappes, X. Wu, J. F. Salazar-Gonzalez, M. G. Salazar, J. M. Kilby, and M. S. Saag.** 2003. Antibody neutralization and escape by HIV-1. Nature **422:**307-312.

156. **Weyengera, M., W. Byarugaba, and H. Kajjumbula.** 2007. Frequency and site mapping of HIV-1/SIVcpz, HIV-2/SIVsmm and other SIV gene sequence cleavage by various bacteria restriction enzymes: Precursors for a novel HIV inhibitory product. African Journal of Biotechnology **6**.

157. **Whitney, J. B., A. L. Hill, S. Sanisetty, P. Penaloza-MacMaster, J. Liu, M. Shetty, L. Parenteau, C. Cabral, J. Shields, and S. Blackmore.** 2014. Rapid seeding of the viral reservoir prior to SIV viraemia in rhesus monkeys. Nature.

158. **World Health Organisation,** HIV/AIDS, Global Health Observatory (GHO). Data and Statistics [Accessed: 22/06/2015]

159. **Willey, S., M. Aasa-Chapman, S. O'Farrell, P. Pellegrino, I. Williams, R. A. Weiss, and S. J. Neil.** 2011. Extensive complement-dependent enhancement of HIV-1 by autologous non-neutralising antibodies at early stages of infection. Retrovirology **8:**16.

160. **Wright, J. K., Z. L. Brumme, J. M. Carlson, D. Heckerman, C. M. Kadie, C. J. Brumme, B. Wang, E. Losina, T. Miura, and F. Chonco.** 2010. Gag-protease-mediated replication capacity in HIV-1 subtype C chronic infection: associations with HLA type and clinical parameters. Journal of Virology **84:**10820-10831.

161. **Wright, J. K., V. L. Naidoo, Z. L. Brumme, J. L. Prince, D. T. Claiborne, P. J. Goulder, M. A. Brockman, E. Hunter, and T. Ndung'u.** 2012. Impact of HLA-B* 81-associated mutations in HIV-1 Gag on viral replication capacity. Journal of Virology **86:**3193-3199.

162. **Wyma, D. J., J. Jiang, J. Shi, J. Zhou, J. E. Lineberger, M. D. Miller, and C. Aiken.** 2004. Coupling of human immunodeficiency virus type 1 fusion to virion maturation: a novel role of the gp41 cytoplasmic tail. Journal of Virology **78:**3429-3435.

163. **Zaitseva, L., R. Myers, and A. Fassati.** 2006. tRNAs promote nuclear import of HIV-1 intracellular reverse transcription complexes. PLoS Biology **4:**e332.

164. **Zolla-Pazner, S., and T. Cardozo.** 2010. Structure–function relationships of HIV-1 envelope sequence-variable regions refocus vaccine design. Nature Reviews Immunology **10:**527-535.